UNIVERSITY OF TARTU
INSTITUTE OF ECOLOGY AND EARTH SCIENCES
DEPARTMENT OF GEOLOGY

PEETER PAAVER

Geopolymeric potential of the Enefit 280 oil shale solid heat carrier retorting ash

MSc. Thesis

Supervisors:
Päärn Paiste
Kalle Kirsimäe

TARTU 2016

Geopolymeric potential of the Enefit 280 oil shale solid heat carrier retorting ash

Up to the present day the amounts of the ash residues coming from the Estonian shale oil industry have been relatively small. However, the shale oil producers in Estonia are shifting their focus to a new and more powerful type of SHC retorts, like the Enefit 280 retort and in the near future the share of oil and consequently waste ash residue production in Estonia will go up. Geopolymeric binders, produced by alkali activation of different solid waste materials, could be one of the solutions to this waste problem that would give some beneficial use to this industrial waste otherwise landfilled/deposited. In the current thesis different kind of mortars, using the Enefit 280 waste heat boiler (WHB) ash from the retort built in 2012, were mixed to study and evaluate the potential use of solid heat carrier ash for geopolymer type mortar and cement production. This was done by comparing a series of alkali activated WHB ashes with the self-cementation properties of the same material obtained upon hydration with plain water.

T150 - material technology, T420 - petrology, mineralogy, geochemistry

Enefit 280, geopolymer, oil shale ash

Enefit 280 tahke soojuskandja tuha geopolümeerne potentsiaal

Tänase päevani on põlevkiviõli tööstusest tulenevad tuhajäätmete kogused võrreldes elektrijaamades tekkiva tuhaga võrdlemisi väiksed. Kuid viimastel aastatel on Eesti põlevkiviõli suurtootjad investeerinud õlitootmistehnoloogiasse ja käivitamas uusi suure tootlikkusega tahke soojuskandja tehnoloogiat kasutavaid süsteeme. Nende tehastega kaasneb paratamatult ka põlevkiviõli tootmisega tekkivate jäätmete hulga kasv. Erineva päritoluga tööstuslike jäätmete leeliselisel aktivatsioonil on võimalik toota geopolümeersed sideaineid-tsemente mis võiksid olla üheks potensiaalsetest kasutusviisidest jäätmetele, mis vastasel juhul leiaksid tee ainult jäätmehoidladesse. Käesolevas uurimistöös selgitati Enefit 280 jääksoojuskatla tuha sobivust geopolümeeride valmistamiseks. Selleks valmistati Enefit 280 tehasest pärineva tuhaga erinevate segudega katsekehad. Tekkinud segude omadusi ja geopolümeriseerumist võrreldi sama tuha ja tavalise vee segamisel tekkivate materjalidega

T150 - materjalitehnoloogia, P420 - Petroloogia, mineroloogia, geokeemia

Enefit 280, geopolümeer, põlevkivi tuhk

Contents

1. Introduction

Geopolymeric binders produced by alkali activation of different solid waste materials as an alternative to common Portland cement are of rapidly growing interest in building materials research all over the world (Provis and Bernal, 2014). This technology applies depolymerization and subsequent repolymerization of aluminosilicate structures of crystalline and amorphous phases under the alkaline treatment, resulting in hardened materials that can result in compressional strength similar to cement binders used for very different applications. Beside the beneficial reuse of solid waste from energetics, ore processing and/or chemical industry it is also of utmost importance that this approach allows significant reduction in the carbon footprint and energy consumption in the production of construction materials with the associated carbon dioxide emissions up to 80% lower (Li et al., 2012) (Provis and Bernal, 2014).

Geoplymeric binders can be produced of any naturally occurring or industrially produced aluminosilicate raw material, such as (kaolin)clay or blast furnace slag from steel industry (Davidovits, 2011). Secondary usage of different industrial by-produces and solid wastes as precursors of geopolymeric binders is specifically beneficial and can significantly reduce the amount of the industrial waste otherwise landfilled/deposited. The raw materials and their processing conditions determine the structure, chemical and physical properties of geopolymeric products formed. In macroscopic scale, geopolymers synthesised from different aluminosilicate sources may appear similar but their microstructure homogeneity and also all other mechanical and chemical properties can vary largely (Subaer and Riessen, 2006).

In addition to different types of slags and the waste from glass manufacturing also e combustion fly ash, a widespread industrial waste, can be potentially useful for production of alkali activated geopolymeric materials. Commonly class F type low-Ca fly ash is used for geoplymeric binders (Zhang et al., 2014). However, also class C i.e. high-Ca fly ashes have been successfully tested for the production of geoplymeric binders (Guo et al., 2010a), (Mijarsh et al., 2015).

Estonian energy sector employs Ordovician marine kerogenous oil shale type fossil fuel, which is a widely-spread sedimentary rock containing kerogenous organic matter that can be pyrolysed to extract shale oil or burnt for heat and power generation (Ots, 2006). Total world

resources of oil shale (as shale oil) are estimated at 4.8 trillion barrels, but production of shale oil is, compared to petroleum, more costly due to mining, processing and environmental costs. Nevertheless, oil shale is processed in several countries world-wide whereas the Estonian oil shale industry is largest in the world with annual mining output in past five years at ca. 14–17 Mt that currently provides about 77% of energy generated in Estonia (Kearns and Tuohy, 2015). The majority (about 80%) of mined oil shale is utilised in thermal power plants for electricity and heat generation, while most of the remaining oil shale (19%) is used for retorting shale oil and shale gas (Ots, 2006).

Oil shale is a Ca-rich solid fuel of low calorific value (Ots, 2006) and the mineral matter content of oil shale can be as high as 80–90 wt%, but it is ca. 40–50 wt% in mined shale beds (Bauert and Kattai, 1997). As a result, ca. 40–50 wt% of the processed shale remains as a solid waste (ash and semicoke). Oil shale ash is a light-colored mineral material that is composed of lime, calcite, anhydrate, different secondary Ca-silicate phases and residual non-carbonate fraction in varying proportions. Composition of the waste depends on processing technology and raw oil shale composition, but the remaining ash is most commonly Ca-rich with CaO content as high as 55% (Bityukova et al., 2010). By its composition oil shale ash is similar to type C fly ash from coal combustion. Oil shale ash has been earlier used for cement, in road construction and for liming in agricultural purposes (Pets et al., 1985; Hanni, 1996), or filter material (Kaasik et al., 2008; Liira et al., 2009a; Kõiv et al., 2010, 2012), the reuse is minimal and most of it (ca. 95%) becomes deposited in large ash fields next to power plants where it solidifies upon hydration and subsequent carbonation (Bityukova et al., 2010; Mõtlep et al., 2010).

The resulting ash plateaus occupy an area more than 20 km^2 and accommodate more than 300 Mt of ash (Mõtlep et al., 2010). The structural, chemical, mineralogical and physical properties (as well as self-cementing) of oil shale ash have been thoroughly studied in the last decades (e.g. Paat, 2002; Kuusik et al., 2005; Liira et al., 2009b; Bityukova et al., 2010; Mõtlep et al., 2010; Pihu et al,. 2012), but secondary use of the oil shale ash has stayed limited, partly due to the lack of suitable alternative applications. Only the finest fractions of the fly ash from thermal power plants with lime (CaO_{free}) content less than 10% are used as an additive to Portland cement whereas shale oil retorting solid residues are currently not used in any beneficial purpose and are landfilled (Bityukova et al., 2010; Motlep et al., 2007).

Retorting of shale oil and gas is performed using either gas as heat carrier or, the most used, solid heat carrier (SHC) process (Motlep et al., 2007). Currently there are two major SHC technology modifications used for shale oil production in Estonia – Petroter technology used at Viru Keemia Grupp and Enefit at Eesti Energia. At the current processing rates, each year 6–8 Mt of oil shale solid waste is produced. Most of it is the ash formed at thermal power plants but ca. 1.5 Mt of shale oil retorting waste is produced annually (Motlep et al., 2007).

Use of oil shale as a fuel for thermal power plants in Estonian is gradually decreasing because of changing energy market and more stringent environmental regulations whereas the production of shale oil is increasing and the retorting of the oil has been foreseen as the main usage of oil shale in coming decades (Liive, 2007). It is therefore important to find sustainable uses for shale oil retorting solid residues and synthesising geopolymeric materials potentially used in building-construction industry is one of the viable options.

Motivation of this study is to find new ways and methods for beneficiary use of oil shale waste, specifically as low-cost building materials. The aim of this thesis is to study and evaluate the potential of kukersite oil shale SHC retorting waste remaining at Enefit 280 shale oil plants for geopolymer type cement and mortar production. The emphasis is given to development of compression strength in alkali activated waste in comparison with the self-cementation of the same material obtained upon hydration with plain water.

2. Enefit 280 solid-heat carrier retorting technology

Two main technologies have been historically used for producing shale-oil in Estonian oil shale industry - the "Kiviter" process and the "Galoter" process. The Kiviter process is conducted in a vertical gas generator (retort throughput 1000 t per day), which is internally heated by combustion of coke residue and non-condensable shale gas. Operation of the Kiviter retort is continuous; whereas the heat is provided by the rising gases, supplemented by recycle gas, burned in the heat carrier preparation chamber. Some additional recycled gas and air are admitted to the chambers near 900 ºC and heat the shale residue to burn off the coke at the last stage of retorting (Soone and Doilov, 2003). Kiviter process results in solid, granular like waste called semi-coke that contains high content of residual organics left due to incompletely retorted organic matter (up to 30 wt%).

The Galoter retorting technology uses spent shale as a heat carrier. The process is based on introducing dried oil shale (<25 mm particle size) into an aerofountain drier where it is mixed with hot (590-650 ºC) shale ash produced by combustion of oil shale semi-coke (at 740-810 ºC under oxygen deficiency) (Golubev, 2003). The oil yield of 11.5-13% in the Galoter process was 3-5% less compared to Kiviter process, but advantages of the Galoter process are: its solid residue (ash) is less harmful to environment, the concentration of organic substances is below 1%; unriched and lower calorific value oil shale can be used (Veiderma, 2003).

Enefit280 technology (as well as Petroter technology used at Viru Keema Grupp AS) is by its nature an enhanced Galoter solid heat carrier technology where during the retorting the oil shale is heated in the absence of oxygen to the temperature (ca. 400 ºC) at which its organic part – kerogen – is decomposed or pyrolysed into gas, condensable oil and solid residue, while the inorganic mineral matrix is retained in the form of spent shale. In the SHC process retorting residue is heated in the air and directed back to the retort as the heat carrier. The main difference of Enefit280 from typical Galoter and the Petroter retorts is its combination with Circulating Fluidized Bed (CFB) combustion unit (Figure 1).

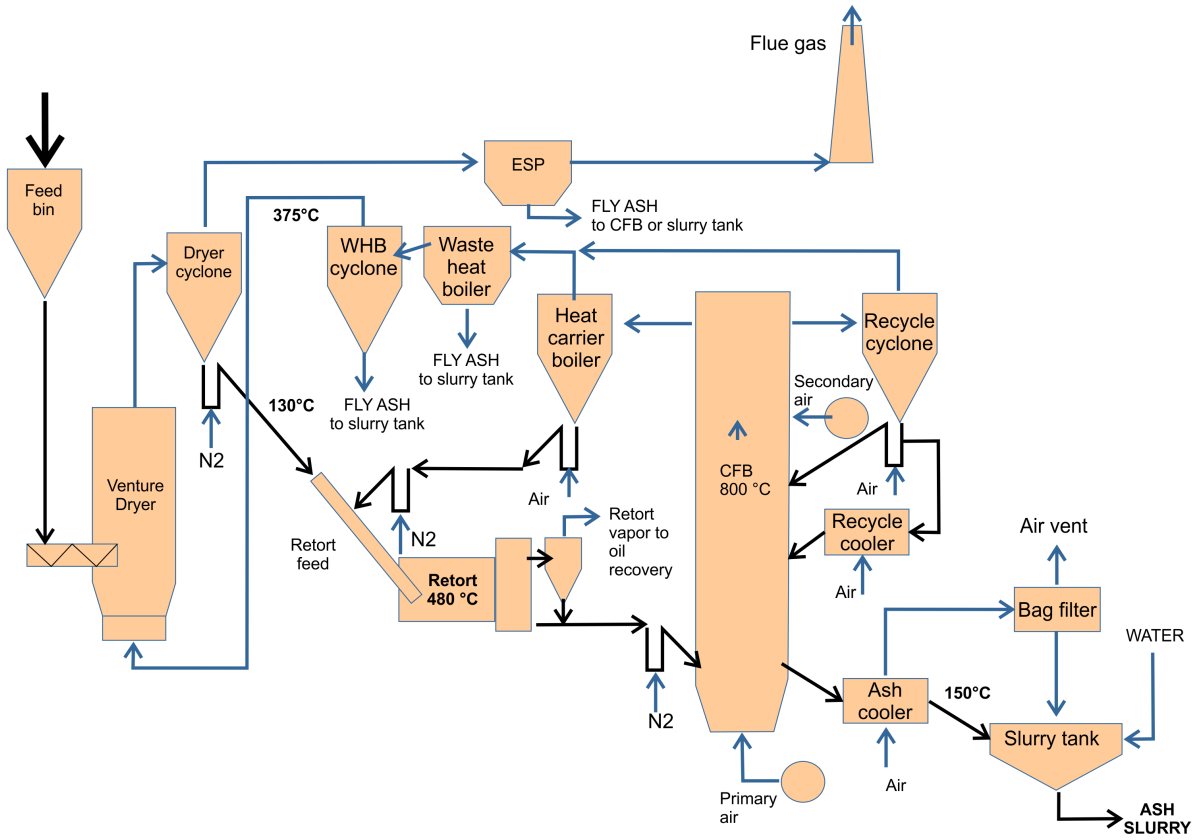

Figure 1.Schematics of Enefit 280 retorting system. Modified after Aarna (2015).

The Enefit 280 system is described in Aarna (2013) and in Enefit 280 retort the oil shale fines (Enefit accepts oil shale fines smaller than 25 mm) are fed into a Venturi-type dryer. Therre oil shale is dried using excess heat of the flue gases that are taken from the system. Oil shale from dryer is further mixed with hot heat carrier ash and becomes fed into a rotary kiln. In rotary kiln the pyrolysis of oil shale takes place. The vapor-gas mixture produced in retort and also the spent shale are separated in two steps in a dust chamber and finally in the downstream cyclone. Vapor-gas mixture is directed to the oil condensation section of the plant. Spent shale from the retort is fed into a Circulating Fluidized Bed (CFB) combustion unit. In CFB unit the spent shale is completely combusted at temperature of 800 °C. Combustion in the CFB allows the system to reduce air emissions efficiently and complete combustion of spent shale (Aarna 2013). As a result the ash resulting from Enefit 280 is free of residual organics. Hot flue gases from the CFB are fed into the Waste Heat Recovery System (WHRS), which extracts excess heat from hot flue gases. The ash in Enefit 280 is collected in different parts of the system and is mixed with water and becomes deposited in waste heaps.

3. Material and Methods

Studied solid heat carrier ash was obtained from the Enefit 280 type SHC retort and was provided by Eesti Energia AS (Estonia). The collected ash represents an average ash feed from waste heat boiler system (WHB). Enefit SHC process results in light-grey to slightly beige retorting ash. Earlier Enefit technology (also the ash produced using Petroter SCH technology at Viru Keemia AS) resulted in dark-grey to black ash residue due to presence of few percent of unburnt organics (Golubev, 2003), (Talviste et al., 2013).

Cementation and geoplymerization of the Enefit 280 ash was studied in 4 series of monolithic samples made by mixing dry ash with the following activators: water, sodium-silicate, sodium hydroxide and sodium silicate + sodium hydroxide (Tables 1-2). The amount of water used in mixtures was equal to the maximum water content in fresh ash at pore space saturation conditions that was determined experimentally prior to the mixing. In addition the amount of water-solution mixed with ash was varied from 45 to 50 vol% in a special test series.

Cylindrical specimens of ash/activator mixtures were prepared and stored in PVC tubes under ambient conditions. For each mixture 3 parallel specimens were made and tested. All sodium silicate based activator solutions were prepared so that the Na_2O content in the additive was 10% (w/w) in order to normalize the added alkaly amount in the mixtures.

Additionally 2 replication series of ash mixed with 50% Na-silicate and NaOH dilution and ash mixed with 1M NaOH were made to study the effects of autoclaving to cementation, during the periods of 14, 24 and 134 hours at temperature of 70 °C and pressure of 2.5 bars.

Self-cementing properties of ash mixtures were evaluated by uniaxial compressive strength tests under continuous loading (20 $kPa \cdot s^{-1}$) until the specimen broke. Compressive strength was measured in three replicas after 7 and 28 days. For testing, cylindrical specimens were removed from the PVC tubes. Altogether 114 compressive strength tests were conducted in the Laboratory of Sedimentology at the Department of Geology, University of Tartu. Mineral and chemical composition of fresh black ash and solidified samples were examined using X-ray diffractometry on Bruker D8 Advance diffractometer using Cu$K\alpha$ radiation and X-ray fluorescence analysis on Rigaku Primus II spectrometer, respectively. The mineral composition of hardening material was analysed in the specimens used in compressive

strength tests, i.e. after 7 and 28 days. Chemical composition was determined from initial fresh ash and samples after 7 and 28 days of curing. The loss on ignition was measured at 950 °C for 2 hours.

For XRD and XRF analysis the materials were dried at 105 °C for 2 hours and ground in planetary ball-mill. The quantitative mineral composition of the unoriented powdered samples was modelled using Rietveld method in Bruker Topas 4.0 code. To determine the quantity of the amorphous glassy phase that is not detected by conventional XRD method, the test specimens were spiked with 10 wt% of ZnO prior to the XRD measurement. Amorphous phase adsorbs X-rays and causes apparent lower ZnO content in sample, relative to the actual spike amount. The amorphous phase content is calculated from difference of added and measured spike phase assuming the alumosilicate composition of the glass.

Scanning electron microscopy imaging of test samples was undertaken on Zeiss EVO MA15 SEM equipped with Oxford AZTEC energy dispersive X-ray analytical system. Samples were analysed both uncoated in variable pressure mode and coated with gold or platinum in high vacuum mode.

4. Results

4.1. Mineral and chemical composition

4.1.1. Fresh Enefit280 WHB ash

Average mineral composition of crystalline phases and an amorphous phase of fresh ash (Figure 2) is dominated by calcite (44.5 wt%), quartz (8.1 wt%) and K-feldspar (7.7 wt%). The content of dolomite is on average 1.0 wt%. All these components are also characteristic to raw oil shale. In addition the WHB ash contained secondary phases formed during thermal treatment of oil shale like authigenic Ca-silicates (11.2 wt%) and periclase (1.0 wt%) but is low (<2%) in $CaO/Ca(OH)_2$.

In comparison with the ash produced in Petrotert solid heat carrier technology at Viru Keemia Grupp AS the most peculiar difference in the mineral composition is the absence of oldhamite phase in Enefit 280 WHB ash. Oldhamite is a CaS phase that is particularly characteristic for Petroter ash and does not occur in thermal power plant (TPP) ashes either (Talviste et al., 2013). Oldhamite forms under oxygen deficiency conditions in reaction between CaO and SO_2. Another mineral indicating oxygen deficiency during Petroter ash formation is partly oxidised Fe-oxide mineral magnetite Fe_3O_4 ($FeO{\cdot}Fe_2O_3$) while in TPP ashes hematite Fe_2O_3 is typically present (Talviste et al., 2013). It is also important that Petroter ash is black/dark grey in colour because the presence of unburnt organic carbon (C_{org}) that ranges between 1.5–2.2 wt% in Petrotert ash (Paaver et al., 2016) whereas Enefit280 ash is grey-beige and does not contain any significant amount of residual organic carbon. This is due to effective burnout during the waste processing in CFB furnance in Enefit280 retorting system where the waste from retort is kept in the presence of excess oxygen at temperatures about 800 °C to allow burnout of all organics left in material after retorting.

The mineral composition of the WHB ash indicates that content of several reactive phases (e.g. lime, belite-C2S) that potentially can react with water and therefore could give to the WHB ash cementitious properties, are low if compared to Petroter ash or any other TPP ash (Bitjukova et al., 2010; Talviste et al., 2013, Paaver et al., 2016). Similar to Petroter ash the Enefit280 WHB ash contains notably low amount (<3%) of lime CaO and/or portlandite $Ca(OH)_2$ suggesting that carbonation reactions do not contribute much to the stabilization of the sediment.

Potentially cementitious phases recognized in WHB ash are secondary Ca-silicate minerals belite/C2S, merwinite, wollastonite and akermanite (Table 2). Belite is a typical phase in cement clinker and its hydration in cement pastes occurs over 60–90 days, but its final strength peaks at about 40 MPa for pure compound (Mindess et al., 2003). However, the content of belite in WHB ash is rather low (<4 wt%) and also the content of other Ca-silicates is low (<12% in total) suggesting rather low uniaxial compressive strength values developing upon simple hydration of the that ash.

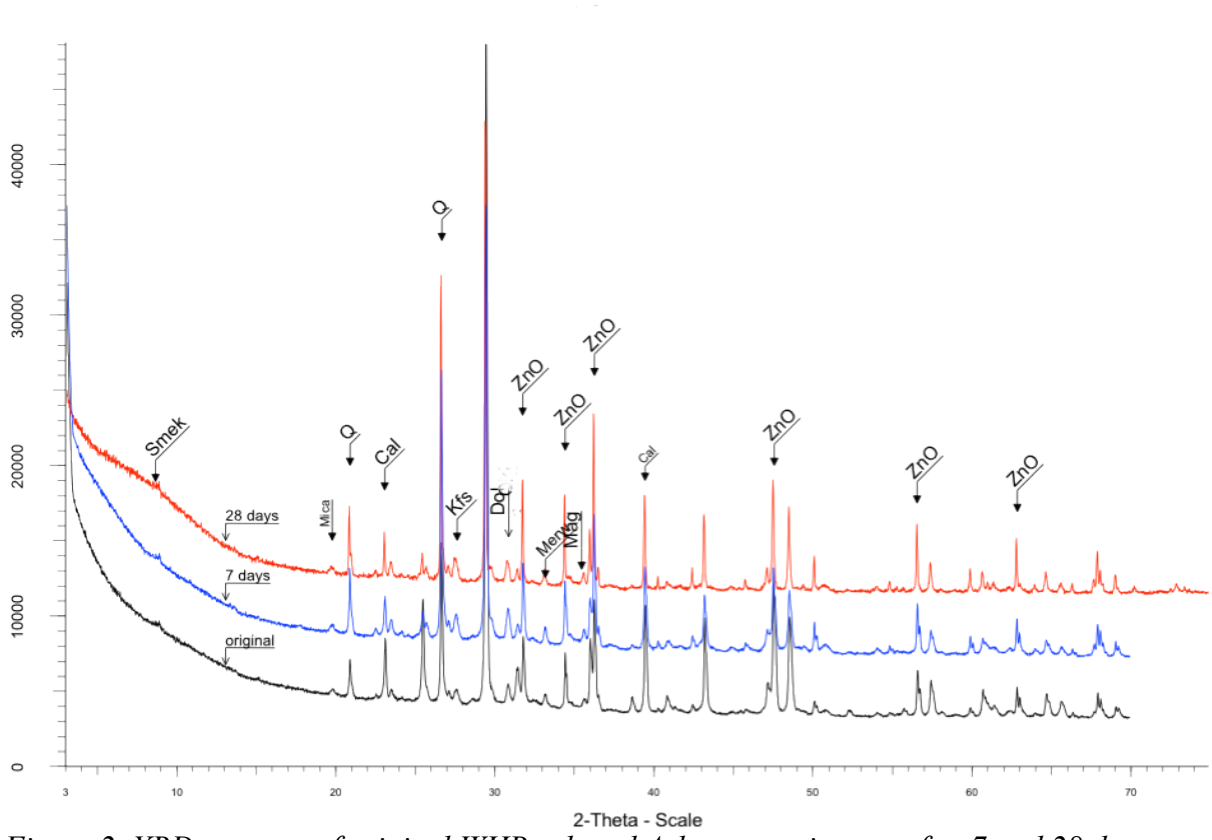

Figure 2. XRD patterns of original WHB ash and Ash-water mixtures after 7 and 28 days., Smek – smectitic clay, Mica – Muscovite. Q – Quartz, Kfs – K-felspar, Cal – Calcite, Dol – Dolomite, Merw – Merwinite, Mag – Hematite/Magnetite, ZnO - Zincite Oxide.

Chemical composition of the fresh ash (Table 4) corresponds to the mineral composition of studied samples and is dominated by SiO_2 and CaO that compose on average 34.1 wt% and 22.2 wt%, respectively. Content of MgO, Al_2O_3 and Fe_2O_3 in fresh ash is on average 3.3, 6.9 and 3.5 wt%, respectively. Content of SO_3 is notably varying and low, on average 3 wt%.

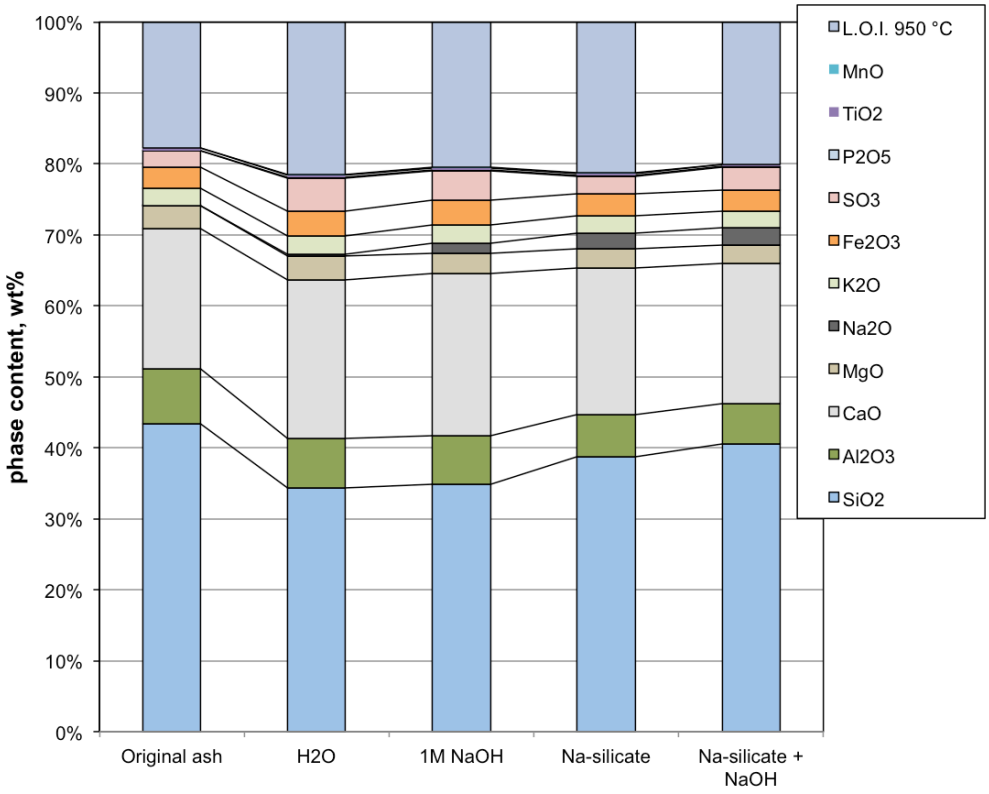

Figure 3. Chemical composition of original WHB ash and all mixtures after 28 days of curing.

4.1.2. Enefit280 WHB ash – water system

Mineral and chemical composition of the WHB and water mixtures is different from the fresh ash composition because of hydration reactions (Figure 2, Tables 2 and 3). Mineral composition of water treated ash samples after 7 days of hydration is similar to the original ash – carbonate mineral phases (calcite and dolomite) content is about 36 wt%. Content of terrigenous mineral phases (quartz, orthoclase and mica-muscovite) is about 40 wt% and content of secondary calcium silicate phases is about 8 wt%, whereas the content of periclase (MgO) is about 1.5% (Figure 4). The major difference in mineral composition of the hydrated samples after 7 days is the disappearance of CaO and portlandite $Ca(OH)_2$ phase and

formation of secondary Ca-Al hydrate phase hydrocalumite and Ca-Al sulphate-hydrate phase ettringite. The content of hydrocalumite and ettringite after 7 days is, respectively 3.7% and 1.4%. There is also a change in the amorphous phase. Content of the amorphous phase in the fresh ash is about 14 wt% and in the 7th day sample about 6 wt%. This might indicate that some part of the X-ray amorphous phase was dissolved and recrystallized into crystalline part, in this case hydrocalumite and ettringite. However, it must be considered that the relative error in amorphous phase measurements can be as high as 30 to 50%. After 28 days the changes in the mineral composition of the water hydrated samples compared to composition of the mixture after 7 days are rather small. Only hydrocalumite has practically disappeared and the relative content of amorphous phase shows increase which indicates that the metastable phases including the Ca-silicate phases and hydrocalumite have started to decompose as indicated by reduction of their share in mineral composition.

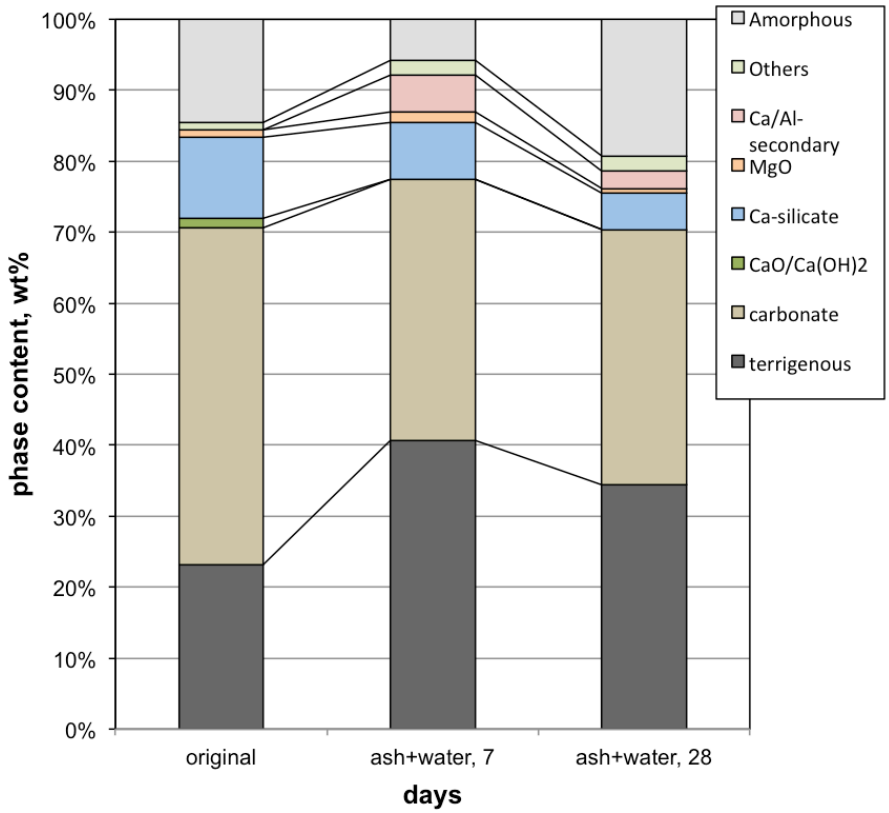

Figure 4.Mineralogical composition of WHB ash and water mixed samples over 7 and 28 days. Terrigenous minerals – quartz, K-felspar, mica/muscovite; carbonate minerals – calcite, vaterite, dolomite; CaO/Ca(OH)2 – lime, portlandite; Ca-silicate – C2S, merwinite, wollastonite; Ca/Al-secondary – ettringite, hydrocalumite; others – magnetite, hematite, gypsum, anhydrite.

4.1.3. Enefit280 WHB ash – NaOH system

Evolution of the mineral composition in samples treated with NaOH activator is similar to the changes in samples mixed with plain water (Figure 5, 6). The content of dominant secondary phases formed in samples treated with NaOH differ compared with water treated samples typically ±5 wt%. However, there are a few specific differences between water mixed and NaOH activated samples. The most important difference compared to the samples treated with water is the absence of ettringite in NaOH activated mixture. Also the content of hydrocalumite is about 3 wt% higher in the 7 and 28 day samples than in specimens mixed with water. In this series, mixed with NaOH, little to no change occurs in mineralogical composition between 7 and 28 day samples.

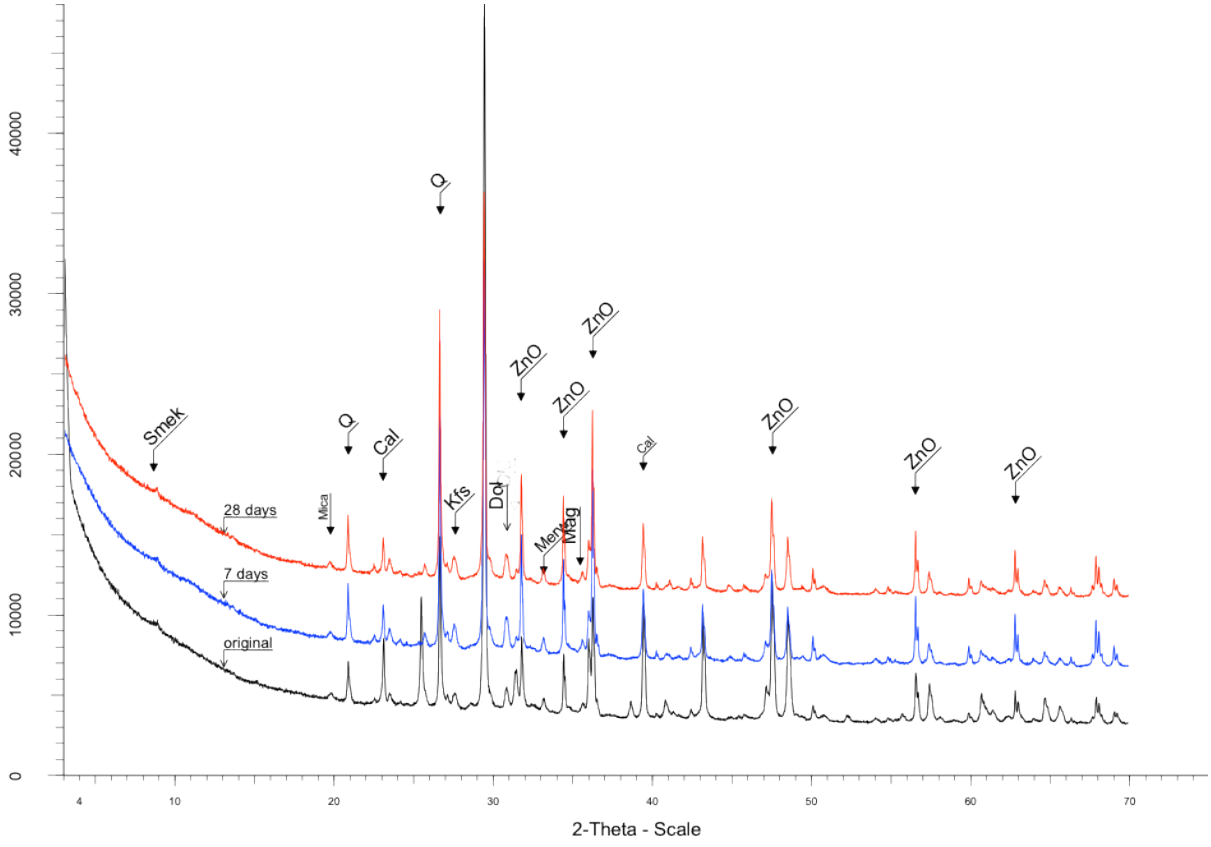

Figure 5. XRD patterns of original WHB ash and 1M NaOH mixtures after 7 and 28 days. For legend, see Figure 2.

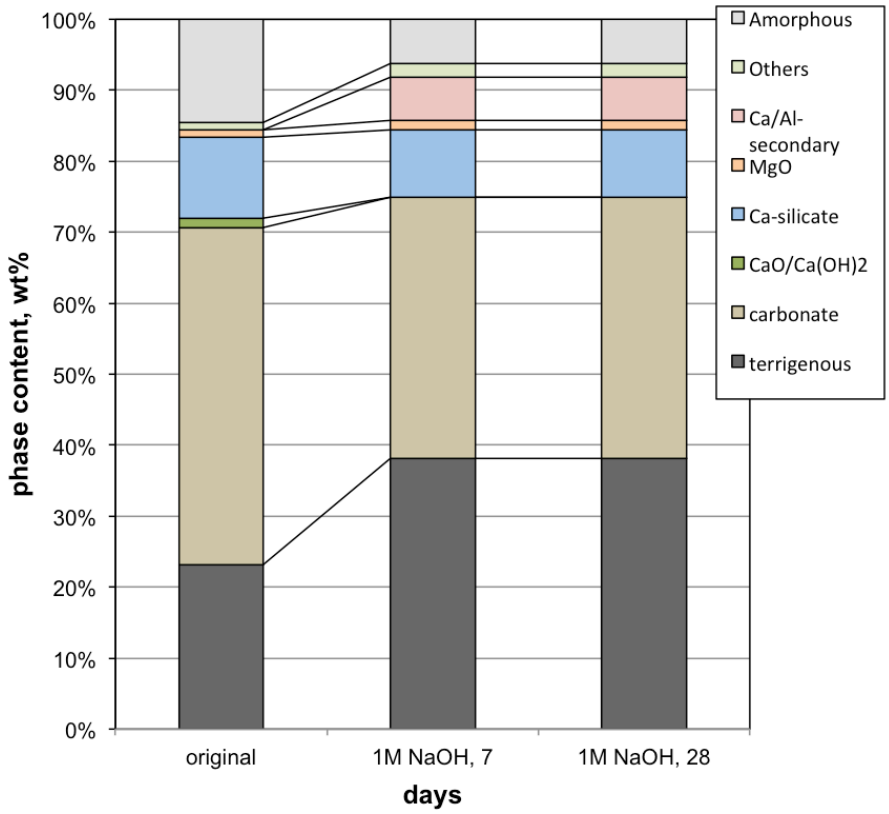

Figure 6. Mineralogical composition of fresh WHB ash and NaOH activated samples over 7, and 28 days. For legend see Figure 4.

In chemical composition the major changes between the fresh ash and NaOH-water mixture after 28 days of curing (Table 2) is exemplified by the increase in Na_2O which is due to addition of NaOH. Similar to ash-water mixture there is also increase in L.O.I. values due to carbonation of portlandite.

4.1.4. Enefit 280 WHB ash – Na-silicate and Na-silicate/NaOH system

Mineral composition of the WHB ash specimens mixed with Na-silicate diluted solution differs considerably from the samples treated with water or NaOH. A distinct and major change compared to fresh ash samples and water and NaOH mixed samples is the content of the amorphous phase, which compared to the 14 wt% in the fresh ash varies from 6 % to 52 wt% in samples mixed with Na-silicate depending on the amount of Na-silicate used, (Figures 7, 8, 15, table 2). This is evidently due to recrystallization reactions and most importantly the formation of amorphous Ca-Na-Al-silicate gel from the reaction between Na-silicate solution and minerals present in WHB ash. As a result of amorphous phase addition there is a decrease in relative content of carbonate phases (calcite, vaterite and dolomite) from 35 wt% of the

fresh ash composition to about 26 wt% in 7 days and also a relative decrease in periclase. It seems that reaction with Na-silicate solution starts to use up the Ca from dissolution of Ca-carbonate phases that indicates formation of amorphous Ca-Silica-Hydrate (C-S-H) phaes in sodium silicate activated samples.

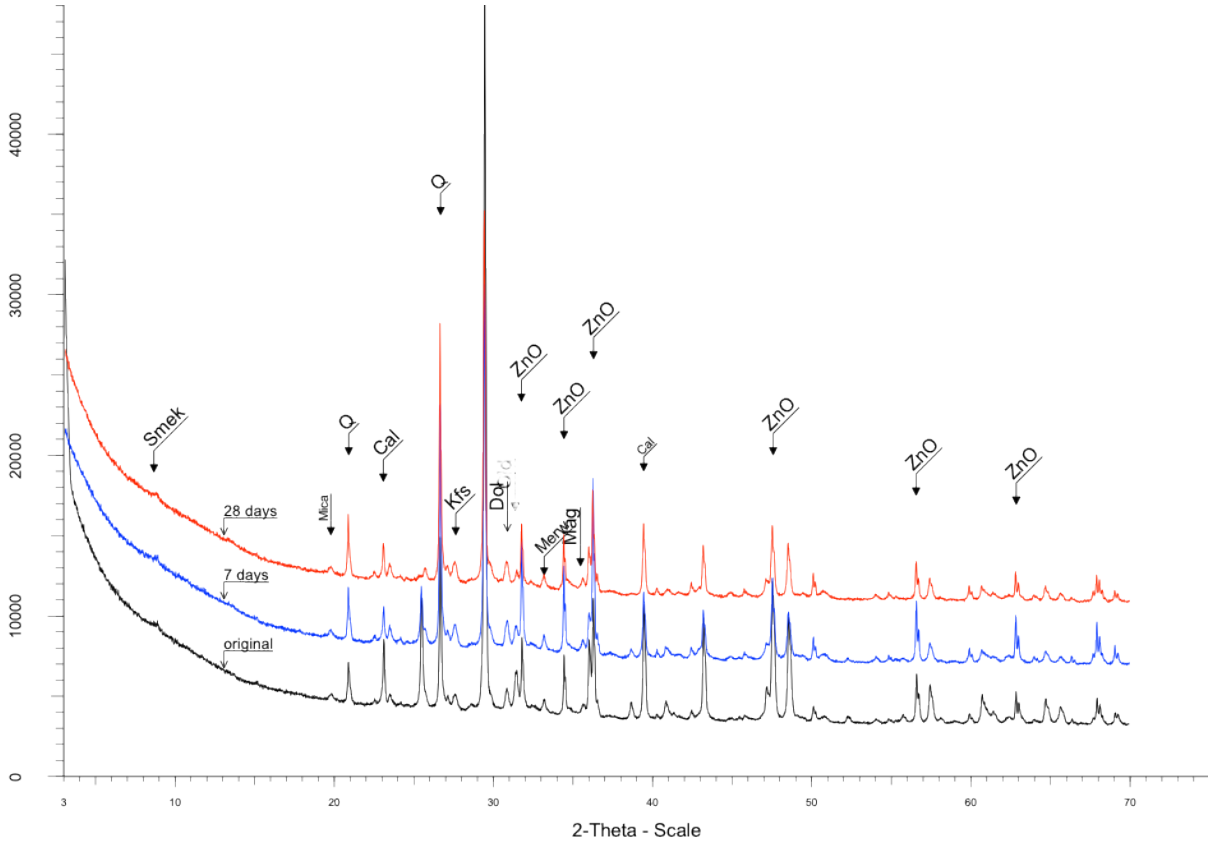

Figure 7. XRD patterns of original WHB ash, 50% Na-silicate dilution and NaOH mixtures after 7 and 28 days. For legend see Figure 2.

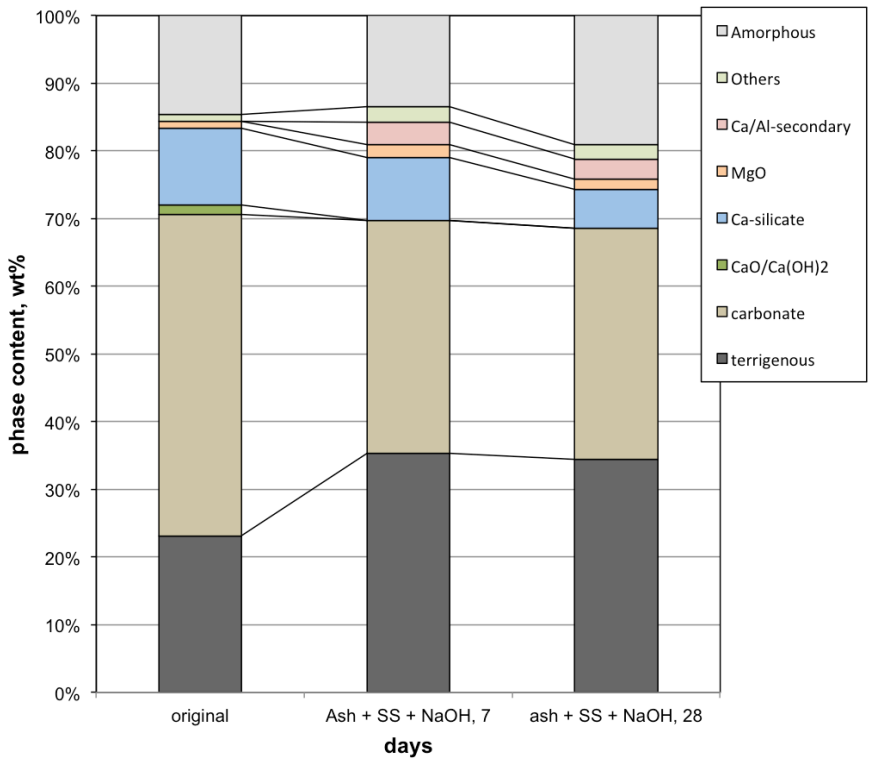

Figure 8. Mineralogical composition of fresh WHB ash, 50% Sodium silicate dilution and NaOH activated samples over 7, and 28 days. For legend see Figure 4.

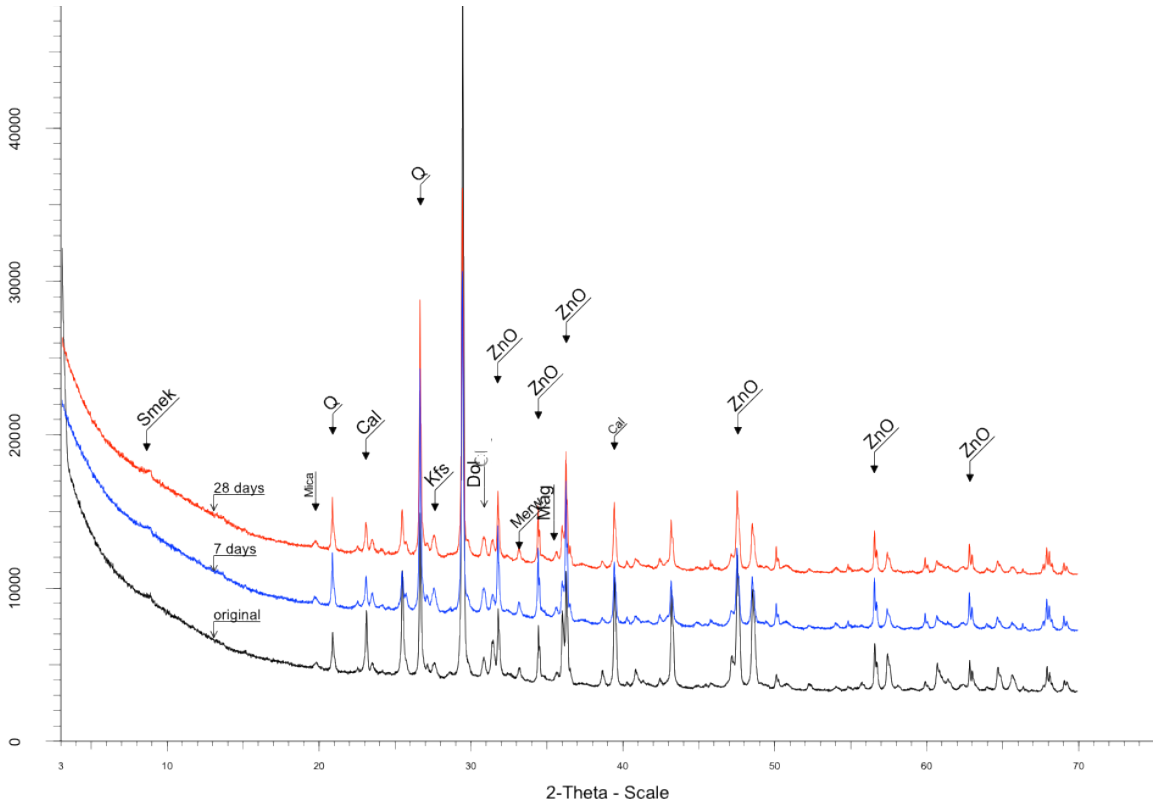

Figure 9. XRD patterns of original WHB ash and 50% Na-silicate mixtures after 7 and 28 days. For legend see Figure 2.

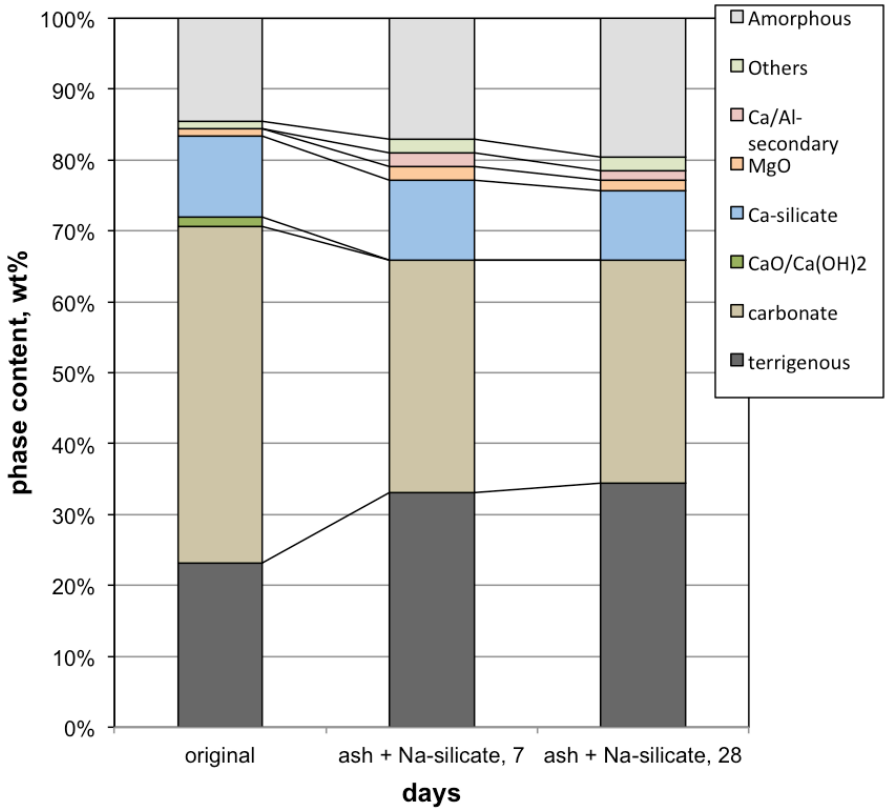

Figure 10. Mineralogical composition of fresh WHB ash and 75% sodium silicate dilution activated samples over 7, and 28 days. For legend see Figure 4.

There are no significant mineralogical differences between samples activated by Na-silicate and samples treated with Na-silicate + NaOH diluted solutions. Differences in mineralogical composition in these two different mixtures vary in the range of a few percent (Figures 6-9, Table 2) indicating similar changes in both mixtures. In chemical composition the observed changes in Na-silicate and Na-silicate/NaOH mixtures compared with original fresh ash are related to addition of Na and Si. In the samples mixed with Na-silicate, SiO_2 content have increased to 32.5 wt% in the sample prepared with Na-silicate + NaOH and 38 wt% in the sample prepared with only Na-silicate.

4.1.5 Autoclaved Enefit280 ash systems treated with NaOH and Na-silicate

4.1.5.1 1M NaOH

Mineralogical composition of the ash and 1M NaOH mixed samples that were autoclaved over 14, 24 and 134 hour time frames and cured after that for 28 days, does not particularly differ from the composition of the samples that were thermally untreated (see Figures 2-9 and Figure 11). Biggest notable change in the mineral composition is the increase in the amorphous phase content from 6.1 wt% in the untreated to 14-21 wt% in autoclaved samples depending on the curing time. The relative increase of amorphous phase content in autoclaved samples possibly indicates that the higher temperature and pressure enhanced the dissolution/amorphisation of the primary silicate phase and also the reaction between Na-silicate gel and Ca-carbonates. However, at prolonged autoclaving for 134 hours the content of amorphous phase shows a decrease that is possibly related to recrystallization and/or decomposition of the C-H-S gel due to carbonation which is indicated by the increase in Ca-carbonate phases at the expense of amorphous material (Figure 11).

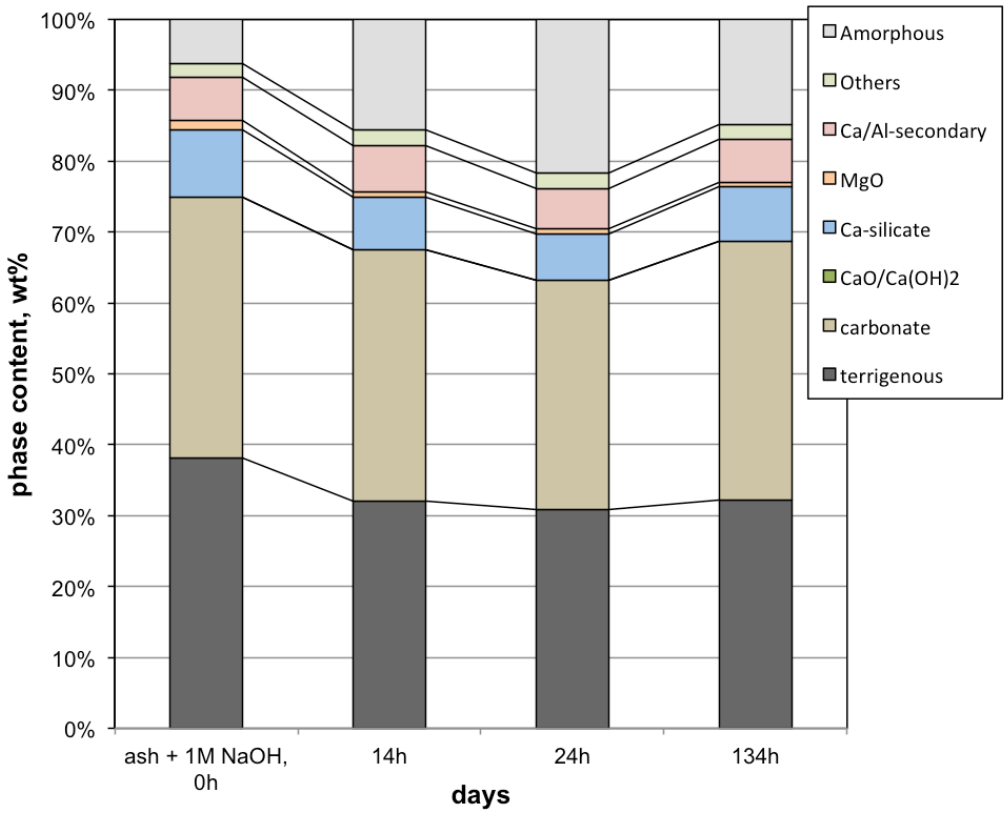

Figure 11. Mineralogical composition of fresh WHB ash and 1M NaOH activated samples, autoclaved for 14, 24 and 134 hours after 28 days. For legend see Figure 4.

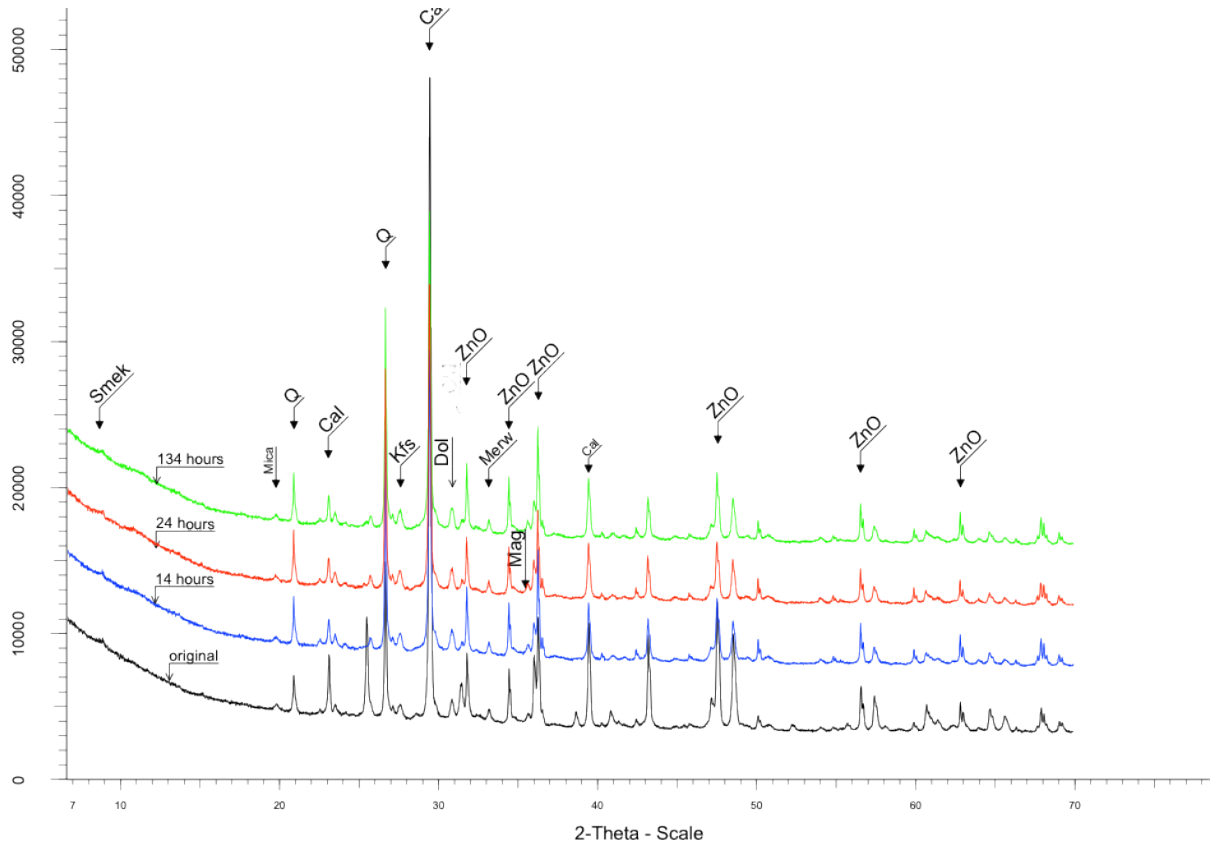

Figure 12. XRD patterns of original WHB ash and autocalved 1M NaOH – ash mixtures. For legend see Figure 2.

4.1.5.2 Na-silicate + NaOH

Unlike the series of ash mixed with 1M NaOH and autoclaved, the autoclaving doesn't affect the composition of samples mixed with Na-silicate and NaOH dilution. A relative rise in amorphous phase content of about 5 wt% could be observed after autoclaving samples for 14 and 24 hours. However, after 134 hours of treatment at elevated temperature it seems that amorphous phase has started partly to crystalize as indicated by XRD results (table 3) showing a drop in amorphous phase to 5.5 wt% from 23.6 wt% in the 24 hour treated sample. Similar effect was observed also in NaOH treated samples where the content of amorphous phase was the lowest in samples autoclaved for 134 hours.

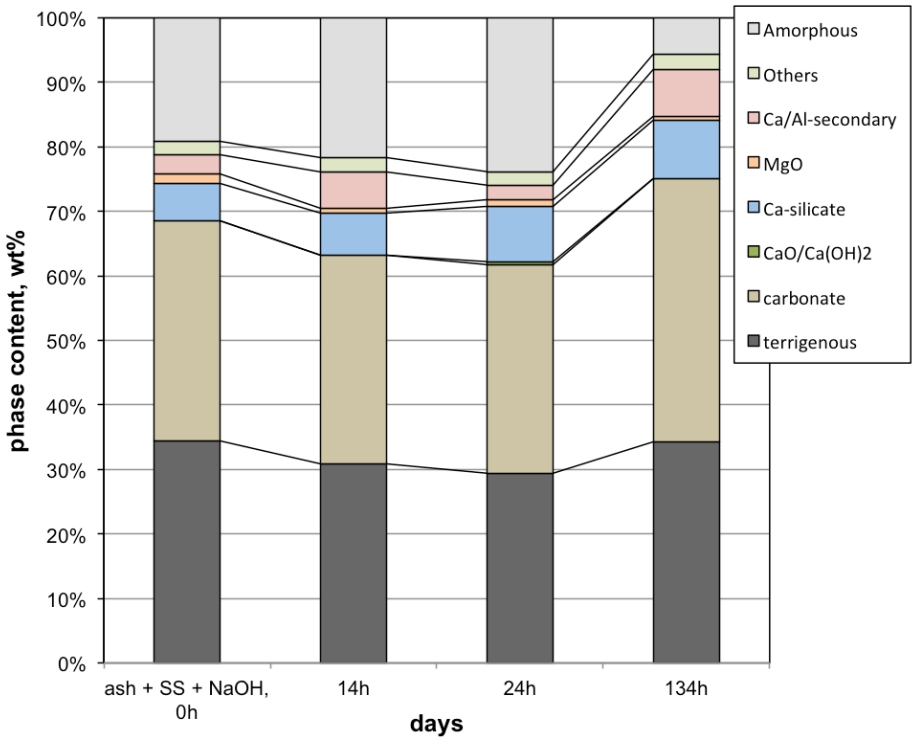

Figure 13. Mineralogical composition of fresh WHB ash, 50% Sodium silicate dilution and NaOH activated samples, autoclaved for 14, 24 and 134 hours after 28 days For legend see Figure 4.

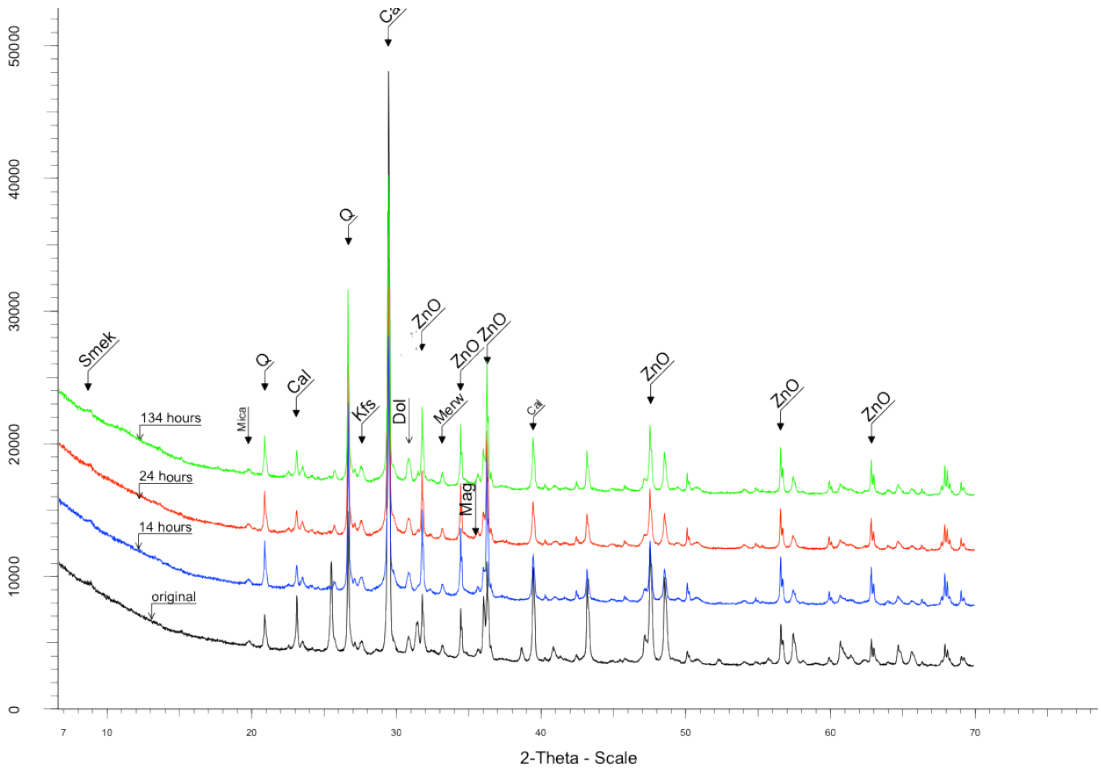

Figure 14. XRD patterns of original WHB ash and autocalved 1M NaOH / Na-silicate + ash mixtures. For legend see Figure 2.

4.1.6 NaOH molarity changes

A sample series of ash mixed with NaOH was made with different NaOH molarity to test the effect of hydroxide concentration on the composition and mechanical properties of the studied materials. Five different sets of replicated samples were made with molarity ranging from 1M dilution to 5M dilution and the composition, as well as uniaxial compressive strength, were measured after 28 days. XRD tests show an increase in amorphous phase content from 6.1 wt% in lowest molarity 1M sample to 21.9 wt% in highest molarity 5M sample. Also the portlandite phase that does not occur in water mixed or 1M NaOH samples, appears in 2M samples and increases together with the increase in NaOH molarity from 1.5 wt% in 2M sample to maximum of 5.4 wt% in 4M samples. This would indicate that part of the Ca dissolved from both Ca-silicate and Ca-carbonate phases is converted under high pH conditions and in presence of excess hydroxide into a portlandite $Ca(OH)_2$ phase.

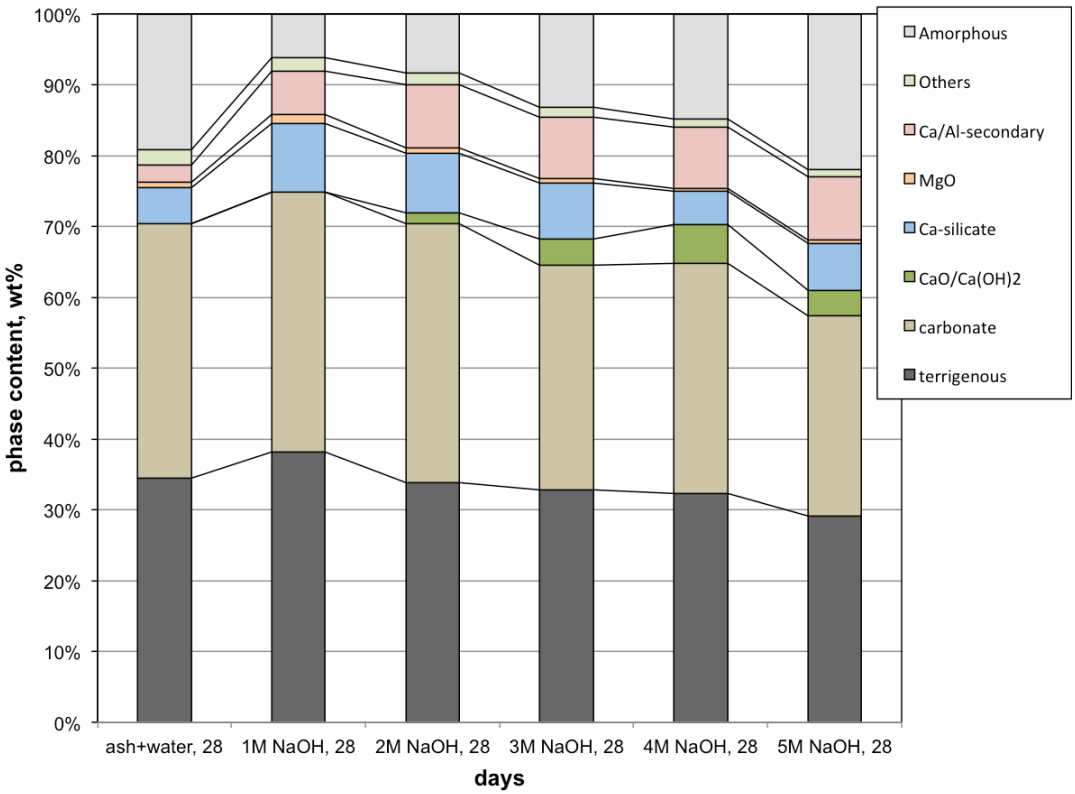

Figure 15. Mineralogical composition of fresh WHB ash + water sample and mixtures with different NaOH molarity after 28 days For legend see figure 4.

4.1.7 Na-silicate volume in dilution

In order to further study the effect of Na-silicate on the compressional strength, two series of samples were mixed with Na-silicate and Na-silicate with added NaOH where the amount of Na-silicate was reduced from level required for 100% saturation of pore space in WHB ash by 25% steps to a minimum of 25%. The 100% saturation level of pores in WHB ashes is achieved when about 60% of water by mass is added to the weight of fresh ash.

In both series overall proportions of the main phases in the mineralogical composition are not affected, at least largely, by reducing the amount of Na-silicate except for the amorphous phase content which is directly correlated to the amount of Na-silicate added to the sample (Figures 16 and 17).

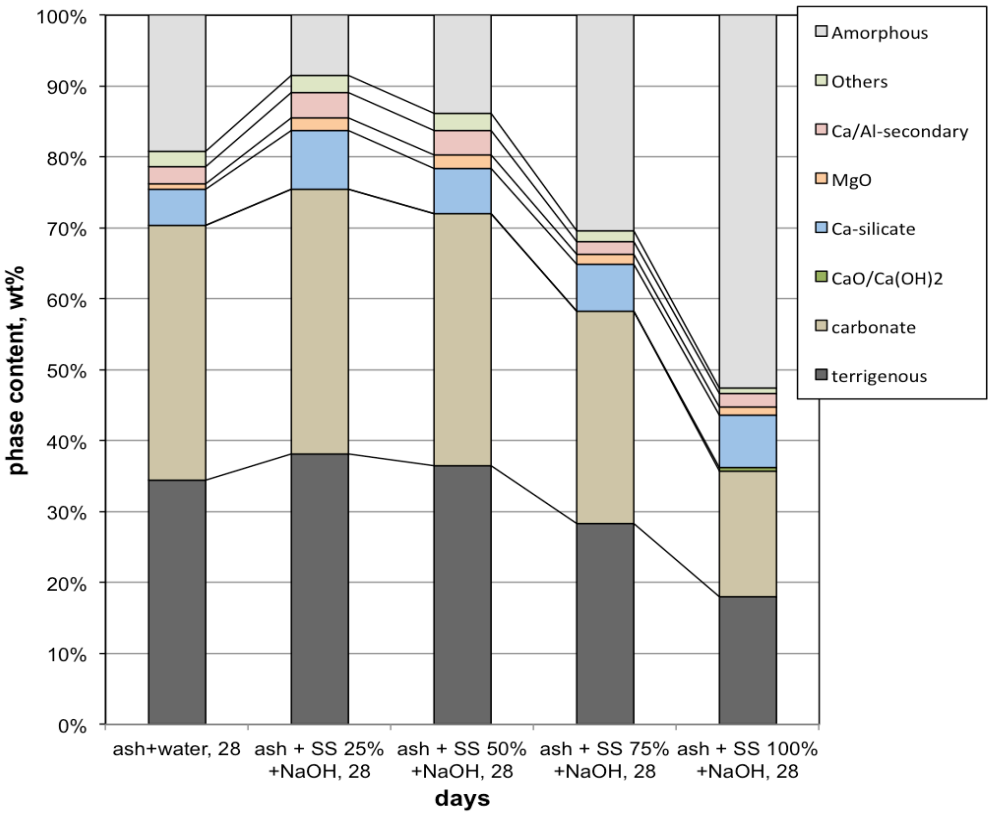

Figure 16. Mineralogical composition of fresh WHB ash + water sample and mixtures with different Na-silicate + NaOH content in dilution after 28 days For legend see figure 4.

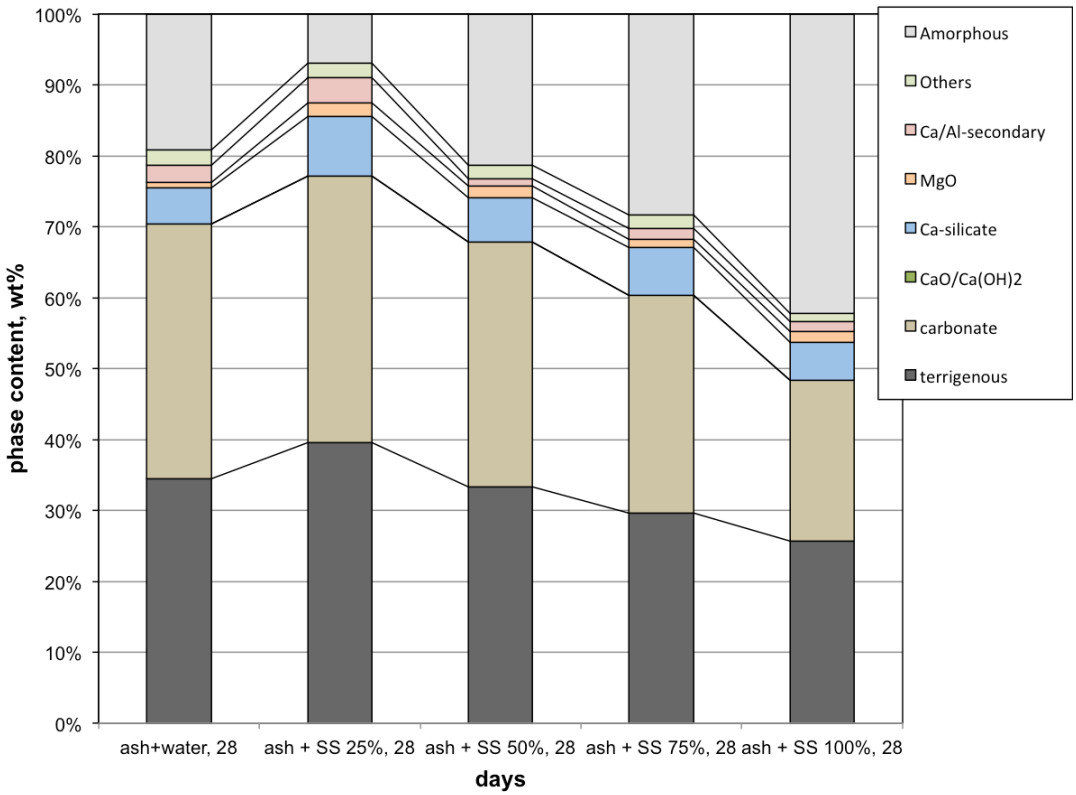

Figure 17. Mineralogical composition of fresh WHB ash + water sample and mixtures with different Na-silicate + NaOH content in dilution after 28 days For legend see Figure 4.

4.2. Microstructure

Scanning electron microscope (SEM) analysis of original WHB ash shows that the material is fine grained with particle size generally less than 100 μm and the material is dominated by fine particles with diameter ~20 μm (Figure 18). The particles are irregular in shape and the finest particles are somewhat aggregated into lumps of 20-30 μm in size (Figure 18b,d).

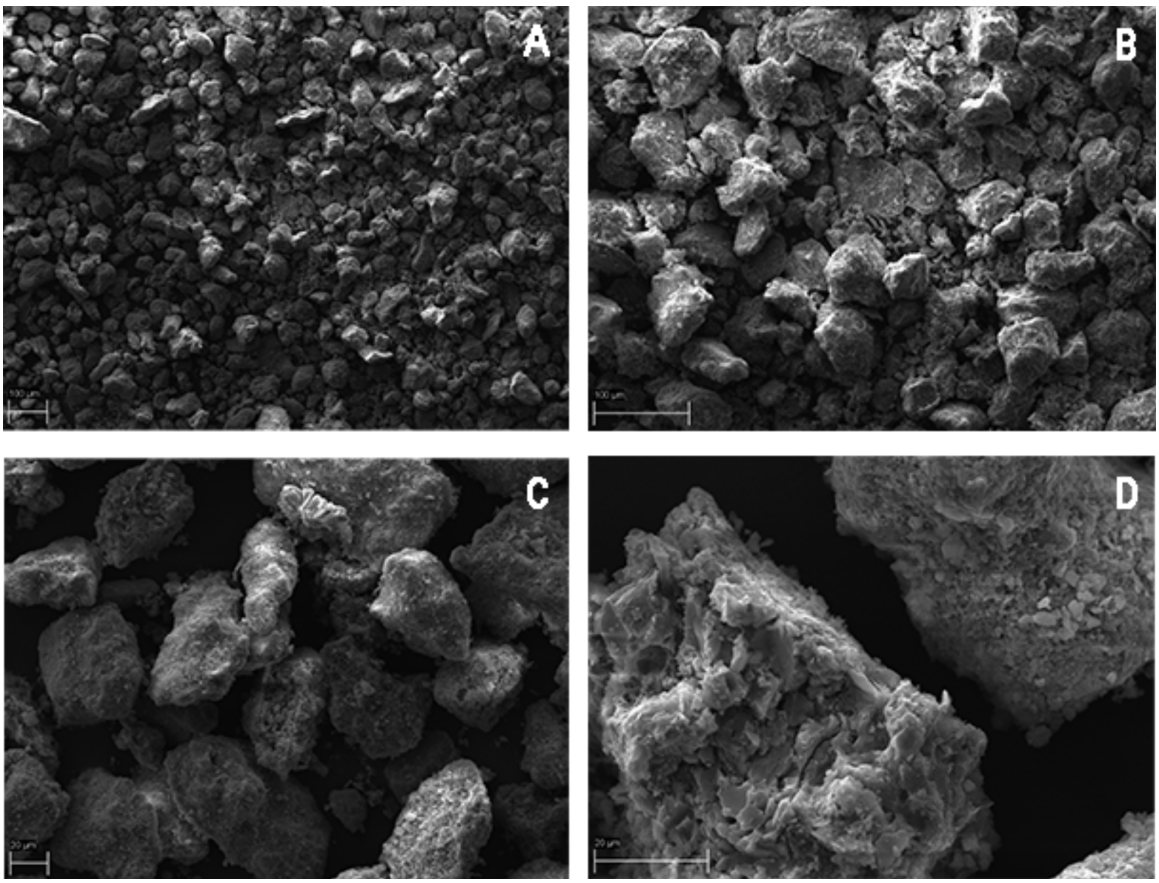

Figure 18. SEM electron images of original Enefit 280 WHB ash.

Samples mixed with water (Figure 19) show intense cementation and development of secondary Ca-Al and Ca-Al-sulphate minerals in the material pore space. The ash particles are covered by secondary precipitates and bonds between particles are generated by interlocking needle and lath-shape authighenic minerals that can be identified by crystallite morphology and chemical composition as hydrocalumite and ettringite. Secondary calcite precipitation can also be observed (Figure 19).

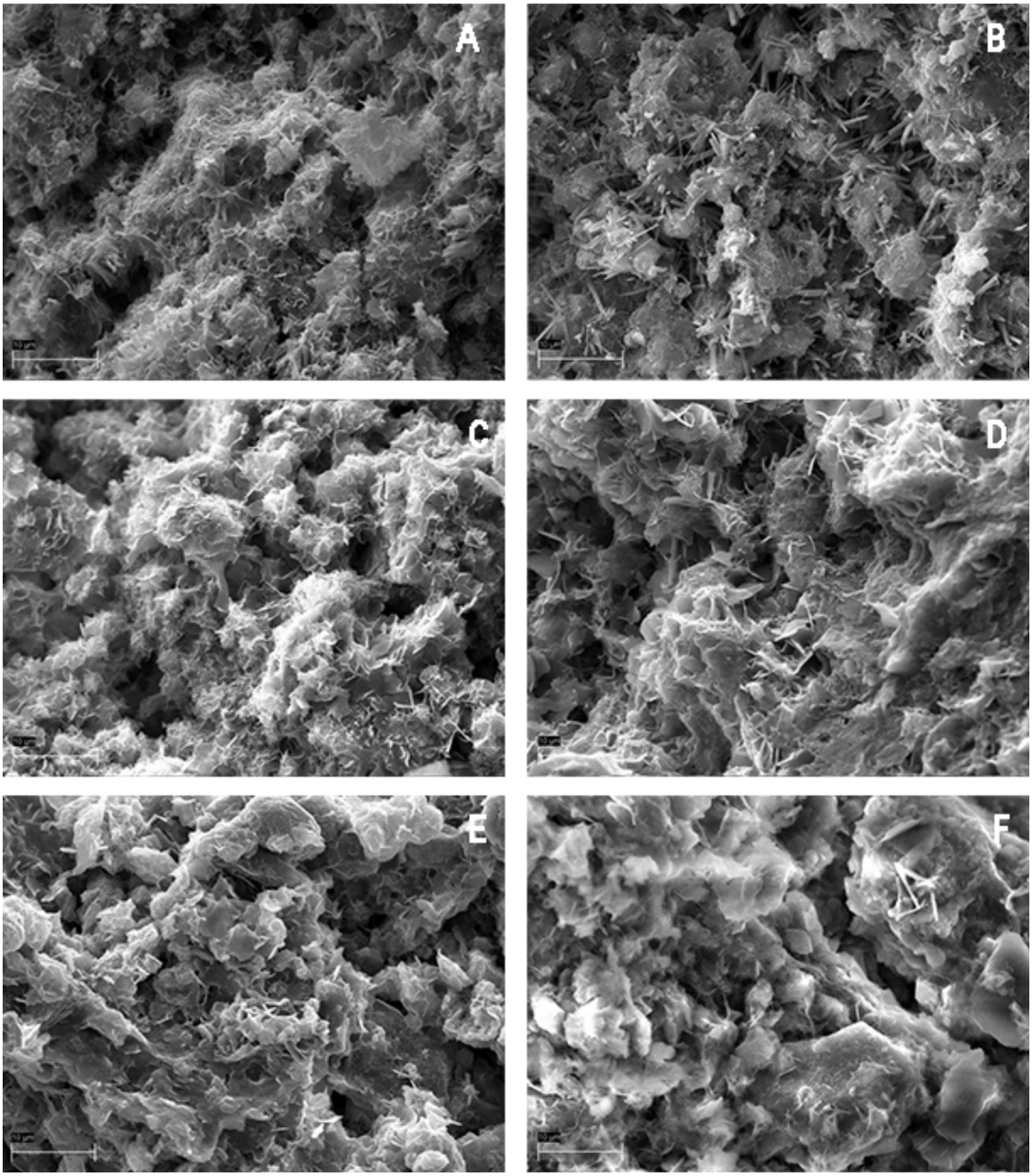

Figure 19. SEM electron images of Enefit 280 WHB ash mixed with water and NaOH after 28 days, A - ash and water, B - ash and 1M NaOH, C - ash and 2M NaOH, D - ash and 3M NaOH, E - ash and 4M NaOH, F - ash and 5M NaOH.

Mixtures activated with only NaOH solution show similar microstructure with water mixed samples (Figure 20), however ettringite is identified only in sample activated with 1M NaOH and the pore-space is filled with hydrocalumite platy crystals and crystal aggregates (Figure 20e, f). This finding agrees well with the mineralogical analysis showing absence of ettringite and presence of abundant hydrocalumite in ash-NaOH system. Size of the hydrocalumite

crystallites is generally 2-5 µm. In sample mixed with 1 M NaOH ettringite formation is similar to that in water mixtures and the pore space is filled with abundant ettringite needles (Figure 20).

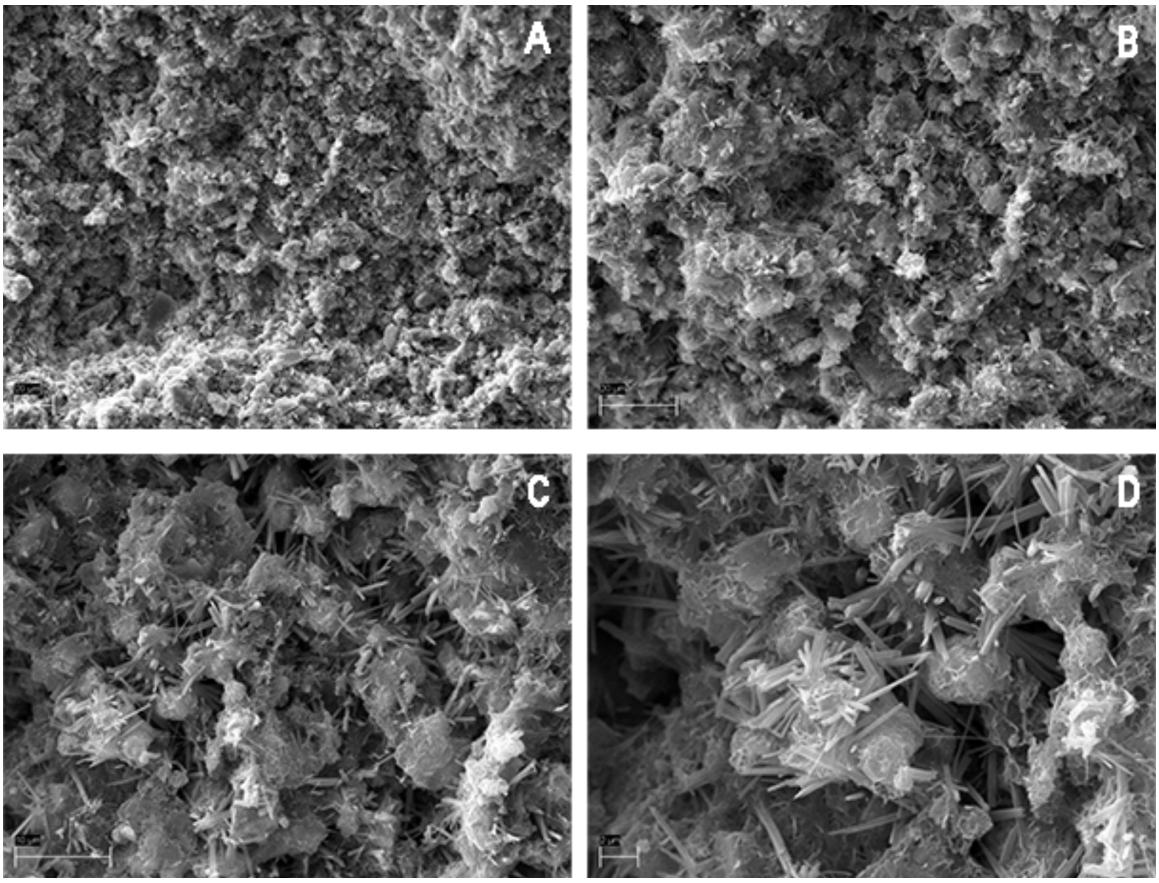

Figure 20. SEM electron images of Enefit 280 WHB ash mixed with 1M NaOH after 28 days. Note abundant pore-filling ettringite in these samples,

Microstructure of Na-silicate/NaOH and Na-silicate activated mixtures is considerably different from water and NaOH mixtures and similar to each other (Figure 21). Under SEM the energy dispersive analysis of the material shows that it is composed of Ca-Na-Al-silicate gel-like matrix that is filling the area between unreacted ash particles. The amount of this Ca-Na-Al-silicate gel as revealed from SEM images shows, however, that in the samples with lower content of Na-silicate admixture the amount of glassy masses is also reduced. This agrees with lower amount of the amorphous phase revealed in XRD analysis of these mixtures.

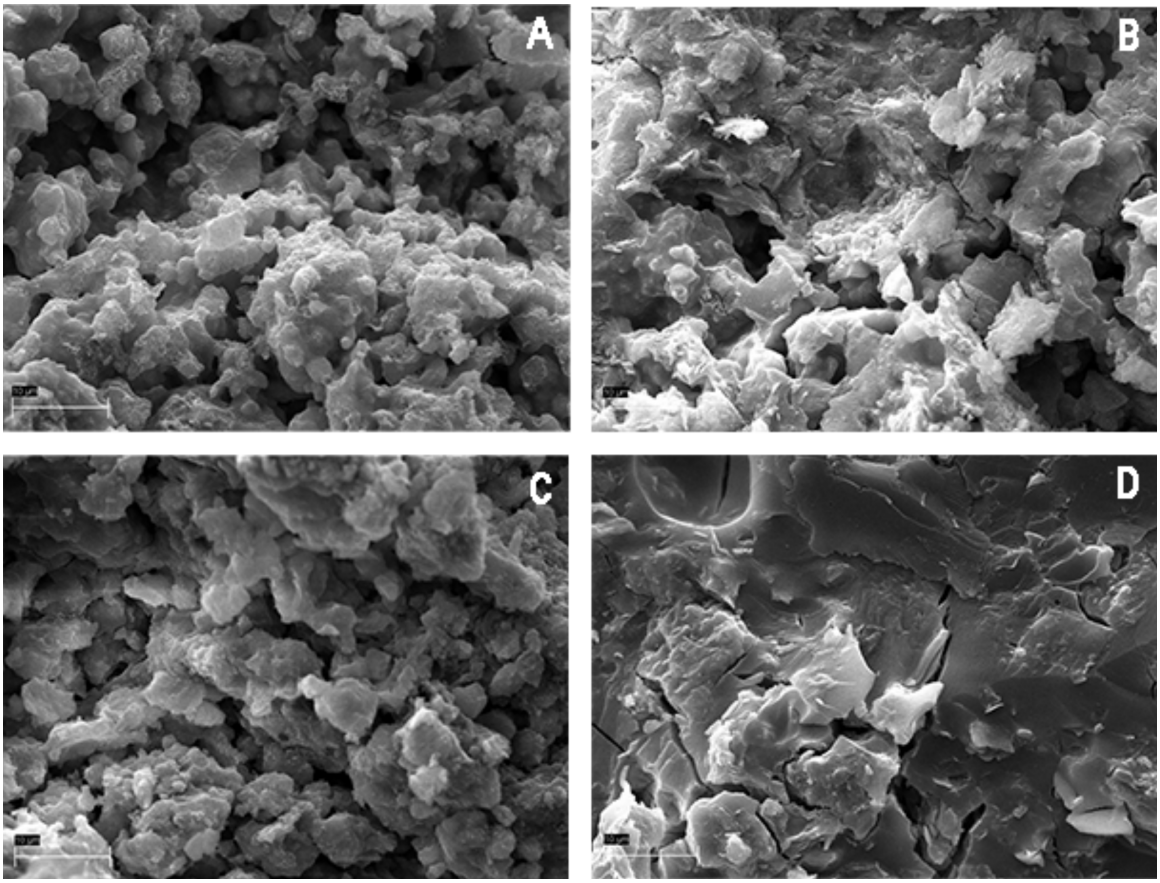

Figure 21. SEM electron images of Enefit 280 WHB ash mixed with NaOH and Na-silicate dilution after 28 days, A – 25% of Na-silicate, B – 50% of Na-silicate, C – 75% of Na-silicate, D – 100% of Na-silicate,

4.3. Uniaxial compressive strength

The Enefit280 WHB ash and plain water mixtures showed uniaxial compressive strength after 7 days of curing on average about 3.5 MPa, and it did not improved much after 28 days of curing yielding values 3.8 MPa on average (Figure 23). In contrast, after 7 days of curing the WHB ash mixed with Na-silicate diluted solution samples and ash mixed with Na-silicate/NaOH diluted solution achieved typically good results in compressive strength (Figures 22 and 23). However, the mixtures made with 25% content of pure Na-silicate activator solution stayed rather weak with uniaxial compressive strength at only 1.2 MPa on average. Nevertheless, most of the samples reached over 4-5 MPa on average and strongest samples were found in mixtures made with 75% Na-silicate solution mixed with NaOH were measured at >11 MPa (Figure 23). Uniaxial compressive strength was measured in 3 replicas in all mixtures after 7 and 28 days and the results are shown in Figures 22, 23, 24.

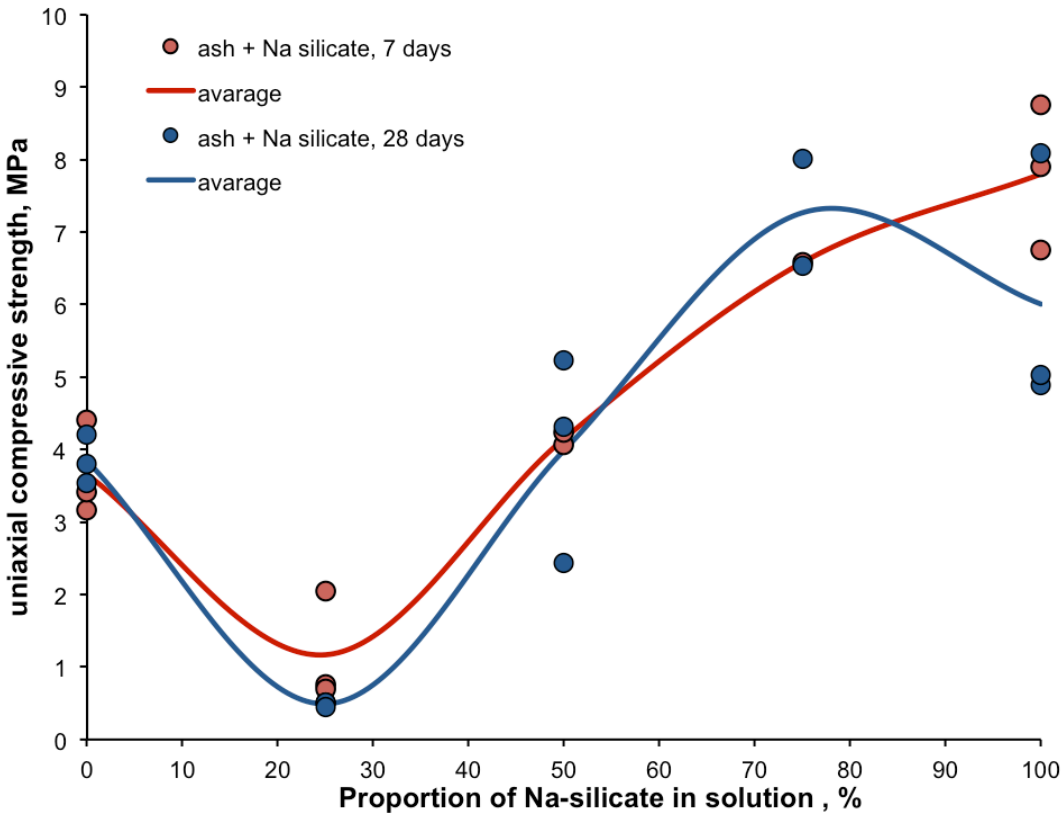

Figure 22. Uniaxial compressive strength of samples mixed with different proportion of Na-silicate in dilution after 7 and 28 days of curing.

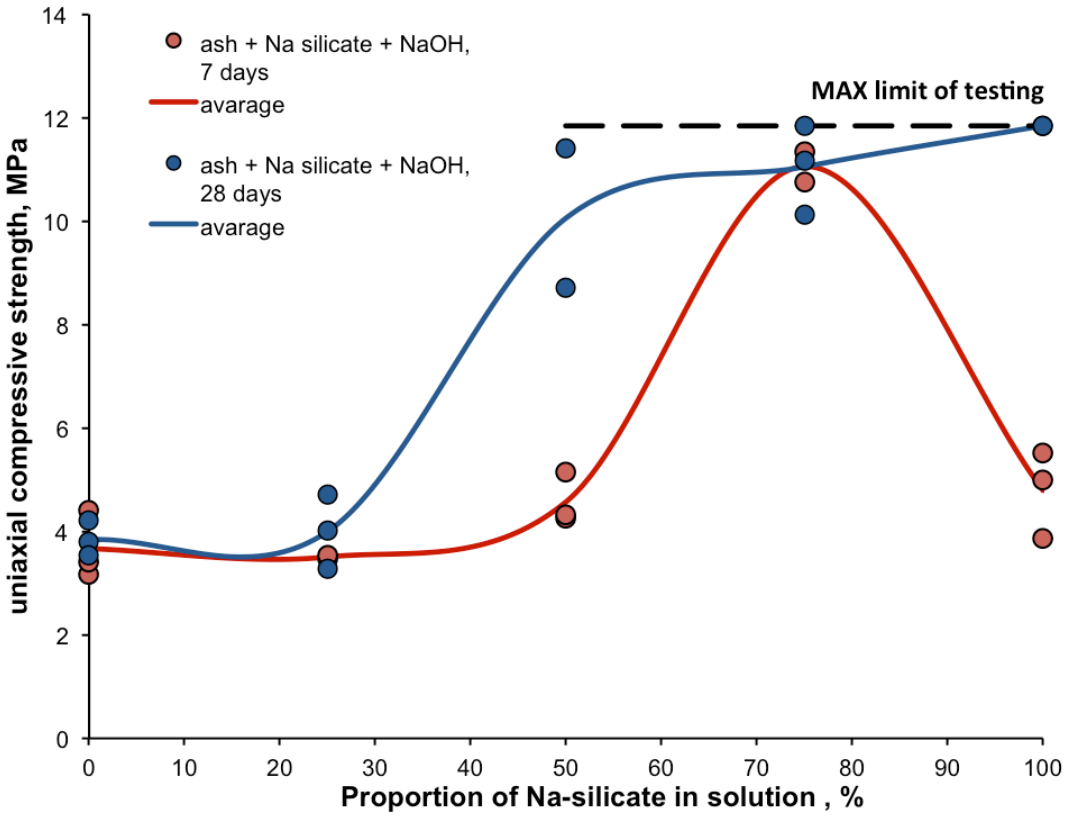

Figure 23. Uniaxial compressive strength of samples mixed with different proportion of Na-silicate and NaOH in dilution after 7 and 28 days of curing

On the other hand, after 28 days of curing the samples mixed with Na-silicate dilutions did not gain any additional strength, and samples mixed with 100% and 25% Na-silicate dilutions were on average even slightly weaker after 28 days of curing.

Samples mixed with Na-silicate + NaOH solution were, compared with water and pure Na-silicate mixtures, significantly stronger. All samples, except the ones mixed with 25% solution, which were in the same range with the ash-water mixtures reaching a maximum of 4 MPa, gained strength over the curing period and reached over 10 MPa on average and peaked at 11.8 MPa, which is also the maximum limit of the uniaxial compressive strength tester used in this thesis.

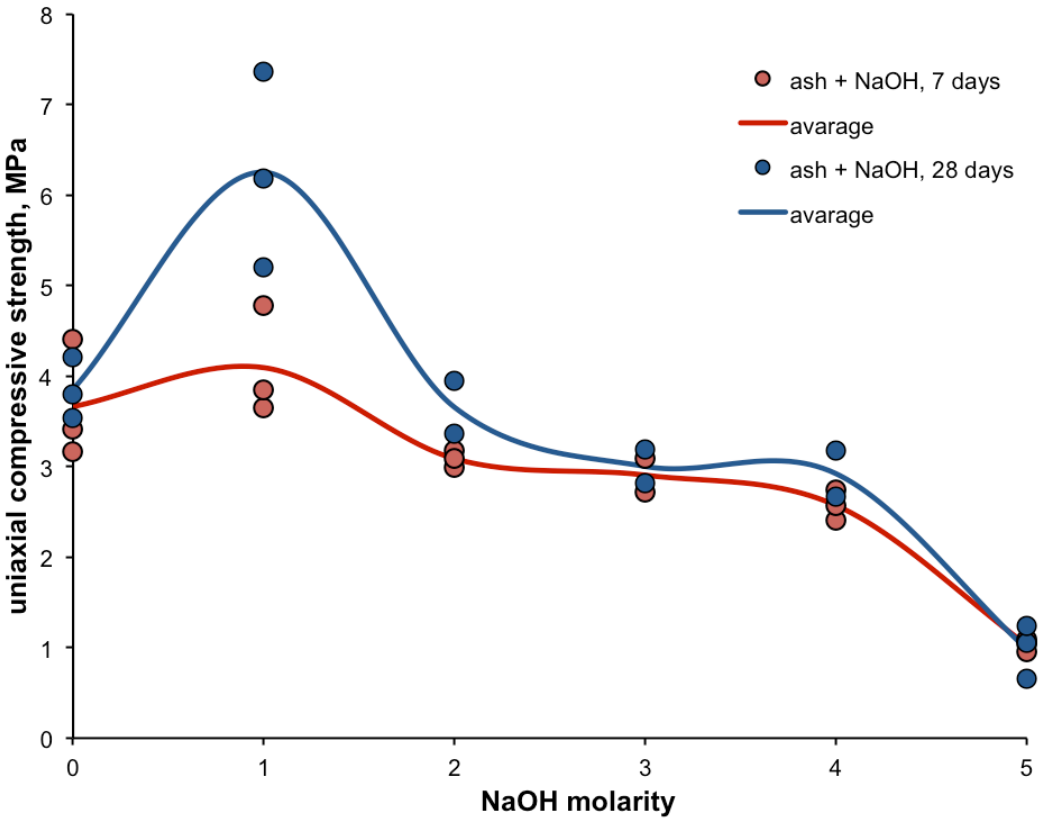

Figure 24. Uniaxial compressive strength of samples mixed with different NaOH molarity after 7 and 28 days of curing

Like the samples treated with Na-silicate and Na-silicate + NaOH diluted solution, most of the samples mixed with water or only NaOH solution did not gain any additional strength over the curing period between 7 and 28 days, except for the series made with 1M NaOH, which reached 4 MPa on average after 7 days and over 6 MPa on average after 28 days. Water, 2M, 3M and 4M NaOH mixtures reached on average 3 MPa in uniaxial compressive strength after both 7 and 28 days and 5M NaOH solution achieved only 1 MPa uniaxial compressive strength on average after the 28 day curing period.

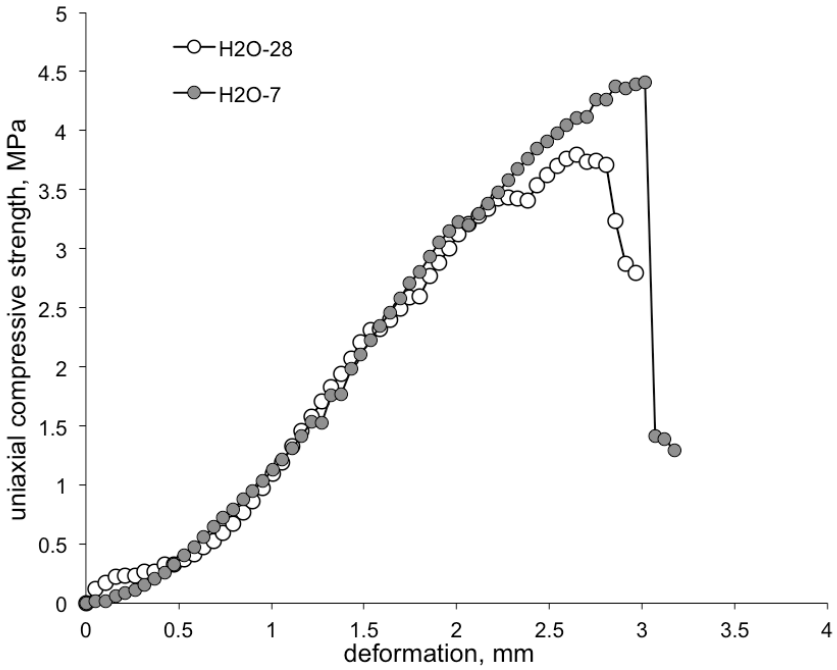

Figure 25. Compressional strength curve of ash and water mixture samples after 7 and 28 days

Compression curves of the Enefit280 WHB ash and plain water mixtures (Figure 25) are characterized after 7 and 28 days of curing at ambient conditions by brittle behaviour of the material whereas there is little difference between the final strength achieved after 7 and 28 days. In contrast, a different compression curves and the development of the compressive strength was observed in samples activated with high molar NaOH activator (>3M NaOH) where high residual strength ("elastic" behaviour) of the material and plastic/ductile deformation after 7 and 28 days of curing (Figures 27 and 28) is observed indicting that no rigid cementation was developed. However, in samples mixed with 1M (figure 26) and 2 M NaOH the samples showed some residual strength after 7 days, but the strength was increased considerably and brittle properties were obtained after 28 days of curing showing higher final strength than in mixture with plain water.

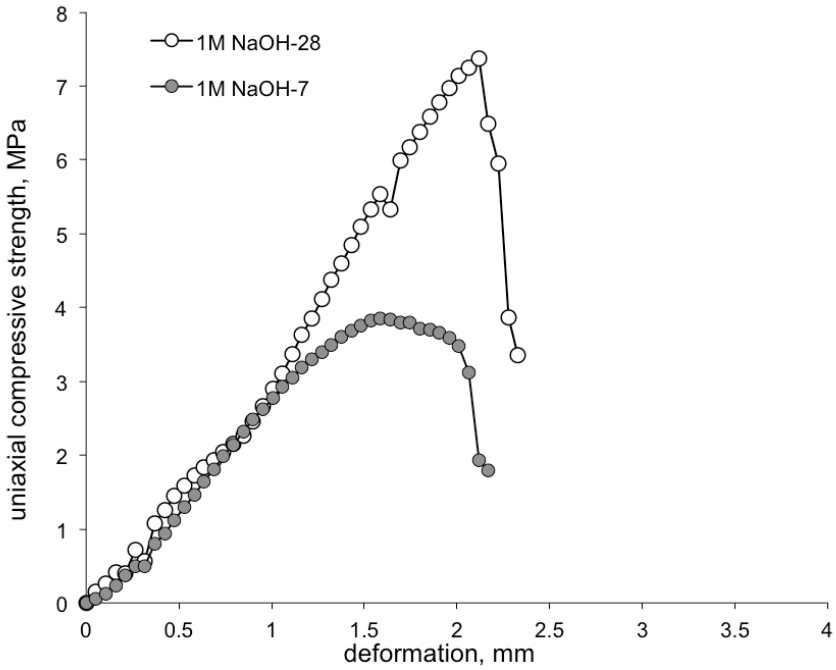

Figure 26. *Compressional strength curve of ash and 1M NaOH mixture samples after 7 and 28 days*

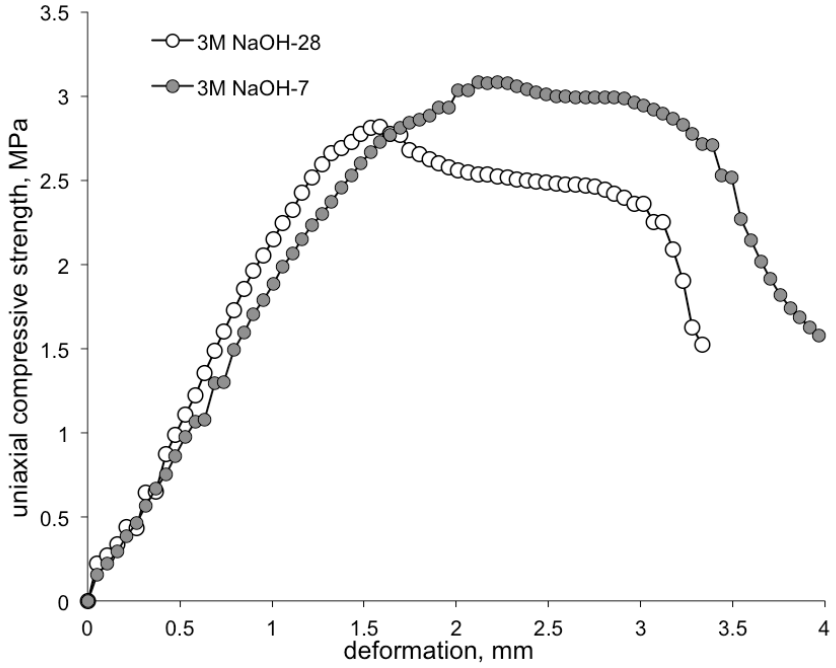

Figure 27. *Compressional strength curve of ash and 3M NaOH mixture samples after 7 and 28 days*

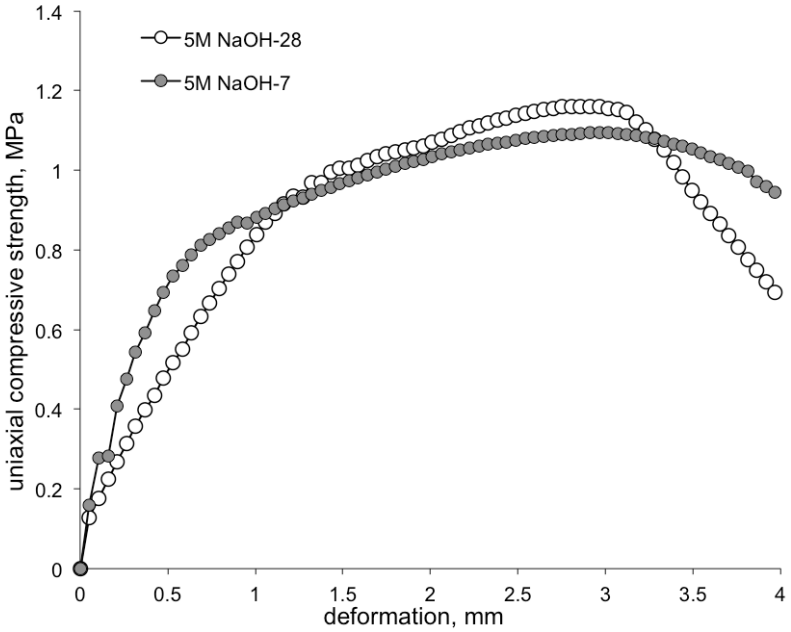

Figure 28. *Compressional strength curve of ash and 5M NaOH mixture samples after 7 and 28 days*

Na-silicate and Na-silicate/NaOH activated samples show remarkably different behaviour compared with mixtures with plain water and the NaOH activated samples (Figure 29). Both mixtures show high strength values and characteristic brittle behaviour already after 7 days of curing and the strength shows increase after 28 days and the samples become more rigid.

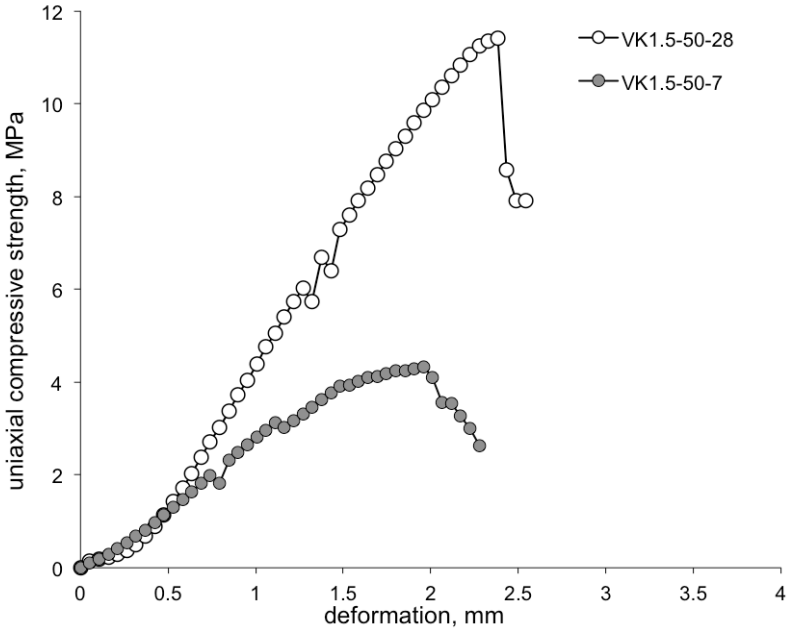

Figure 29. *Compressional strength curve of ash and 50% Na-silicate/NaOH dilution samples after 7 and 28 days.*

Autoclave treatment of Enefit 280 WHB ash mixed with 50% Na-silicate and NaOH dilution and ash mixed with 1M NaOH during the periods of 14, 24 and 134 hours at temperature of 70 °C and pressure of 2.5 bars had significant effect on uniaxial strength development. In mixtures with 1M NaOH the autoclave treatment resulted in significantly lower uniaxial compressive strength after 28 days compared with the strength developed during the same period of time in ash - 1M NaOH mixtures under open air conditions (Figure 30). Also, if the ash - 1M NaOH mixtures without autoclave treatment showed characteristic brittle deformation indicative of cementation, then after autoclave treatment the mixtures exhibited residual strength and plastic behaviour after 28 days of curing. In contrast, the Enefit 280 WHB ash samples mixed with 50% Na-silicate developed in all cases, after treatment for 14, 24 and 134 hours, strong specimens with uniaxial compressive strength exceeding that of the same mixtures without autoclaving and reaching values >12 MPa (Figure 31), that was the maximum pressure attained with the tester used in this study, and the compression curves indicate brittle characteristics that suggests strong cementation of the material.

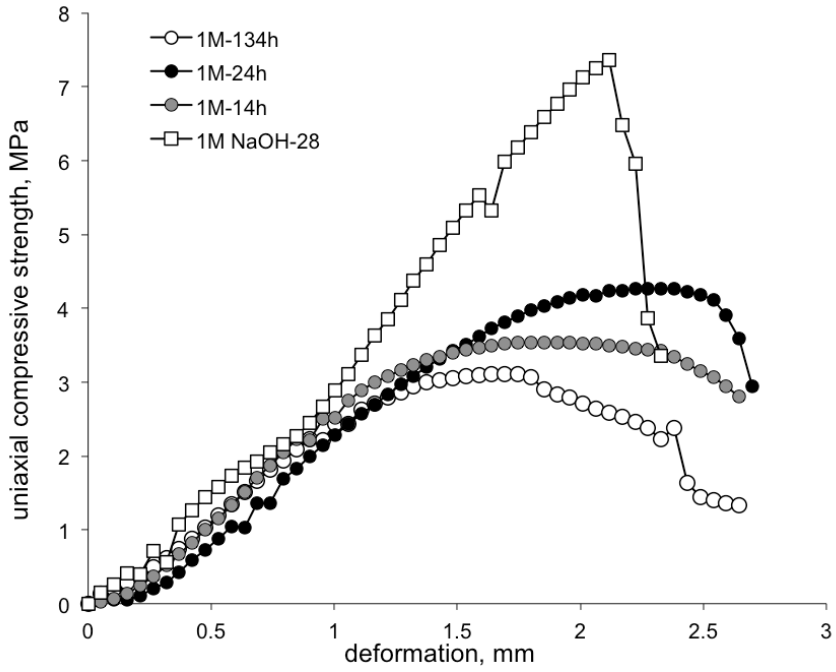

Figure 30. Compressional curves of autoclaved ash and 1M NaOH samples after 28 days

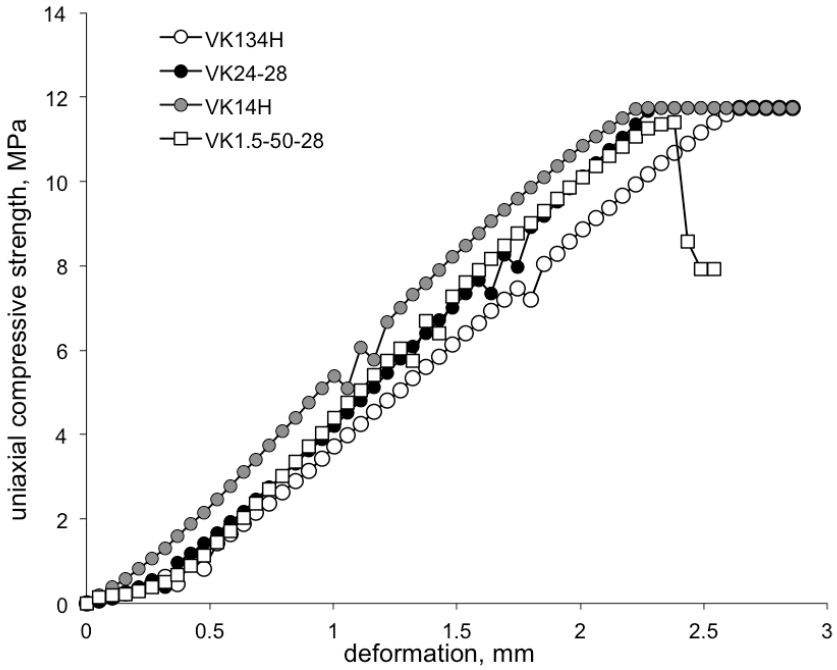

Figure 31. Compressional curves of autoclaved ash and 50% Na-silicate/NaOH dilution samples after 28 days

5. Discussion

5.1 Hydration-geopolymerization and the development of the strength

Fresh WHB ash contains several reactive phases that are capable of reacting with water and/or NaOH, and Na-silicate to form cementitious bonds in the material. However, development of the cementation and buildup of the compressive strength is principally different in mixtures made with plane water and in activated materials. In mixing with plain water, several hydration reactions occur. First of all, the free CaO(lime) reacts quickly with water, forming portlandite $Ca(OH)_2$. In open conditions where atmospheric CO_2 can enter the material the portlandite reacts and secondary Ca-carbonate is precipitated as indicated in mineralogical changes as well as observed in scanning electron microscopy analysis of WHB ash – water mixtures. In water-mixed samples the secondary Ca-Al-sulphate phase (ettringite) and Ca-Al-phase (hydrocalumite) also started to precipitate. Formation of ettringite and hydrocalumite is a characteristic process in hydrated oil shale ash and semi-coke deposits (Motlep et al., 2007), (Motlep et al., 2010), (Sedman et al., 2012a), (Sedman et al., 2012b), (Kuusik et al., 2012). Sulphate needed for ettringite formation was possibly delivered by anhydrite $CaSO_4$ dissolution. However, with overall low content of sulphate and also CaO/portlandite the content of ettringite measured in water treated samples was not very high (max 2 wt%) In comparison, the hydration of oil shale ash from thermal power plants (TTP) and the semicoke waste from shale oil retorting processes typically results in high ettringite content that can reach up to 30 wt% of crystalline phases (Motlep et al., 2007). Similar low content of ettringite upon hydration with water was observed in Petroter ash where ettringite is nearly absent (Talviste et al., 2013) or was found to occur in low content <5 wt% (Paaver et al., 2016). Nevertheless, ettringite plays an important role in self-cementation of semi-coke and power-plant deposits by forming interlocking meshes of needle-like crystals filling the pores space which is evident from SEM analysis of the Enefit280 WBH ash water and 1M NaOH mixtures. Both the secondary Ca-carbonate precipitation and ettringite formation require access of atmospheric CO_2 and some time. However, the ettringite is a stable phase only at elevated pH levels (pH 9-13) and is slowly dissolved by percolating unsaturated precipitation water and becomes replaced by calcite and Ca-sulphate hemihydrate phases meaning that ettringite-based cementation developed in ash-water reactions is not stable in open atmospheric environment in long term.

Mineralogical composition as well as the development of compressive strength in Enefit WBH ash samples activated with NaOH dilution is at first rather similar to the samples mixed with water, though the final strength is lower and it is achieved more slowly, and there is no ettringite observed in XRD nor SEM analysis in mixtures with high molar solutions. It is possible that the lower compressive strength values of the samples activated with strong NaOH specifically in the first stages of the experiment and in final values compared with water mixtures are due to absence of needle like ettringite and/or Ca-monosulphate crystallites that in ash-water mixtures form a rigid connection between ash particles. In high NaOH molar concentrations where pH ~14 is maintained, the ettringite formation depends upon the activity of calcium in solution whereas the formation of calcium hydroxide and sodium-substituted monosulfate phase competes with ettringite formation (Clark and Brown, 1999).

In Enefit280 ash systems it is evident that due to the presence of reactive Ca phases the Ca activity is high and with strong NaOH solution additions the ettringite precipitation is supressed. Ettringite formation was detected in significant amount only in the 1M NaOH – ash mixtures, and these mixtures yielded also the highest strength after 28 days of curing in water – NaOH mixed systems. In strong NaOH solutions, instead, hydrocalumite and possibly some amorphous gel-like material form as evident form increase of amorphous phase with increasing molarity of the NaOH (Figure 33). This gel and the platy crystals of dominant cementitious secondary hydrocalumite, however, do not provide the similar interlocking and overall strength as the ettringite meshes. In mixtures with 1M NaOH most of the matter is in crystalline state, both ettringite and hydrocalumite and secondary carbonate are present and provide the strength of these mixtures.

Geopolymerisation with formation of Ca-Al-Si amorphous matrix and development of high compressive strengths is evident in Na-silicate and Na-silicate/NaOH activated samples. However, the behaviour of these samples is remarkably different form the ash and water mixture, and also the NaOH activated samples. Both of the Na-silicate containing mixtures show high strength values with increasing activator content values whereas it seems that addition of low quantities of activator does not improve the cementation, but results in lower uniaxial strength values compared to ash – plain water mixtures. The good compressive strength of these mixtures is evidently provided by Ca-Na-Al-silicate gel formation in the pore space of the ash aggregate as evidenced from SEM and XRD analysis.

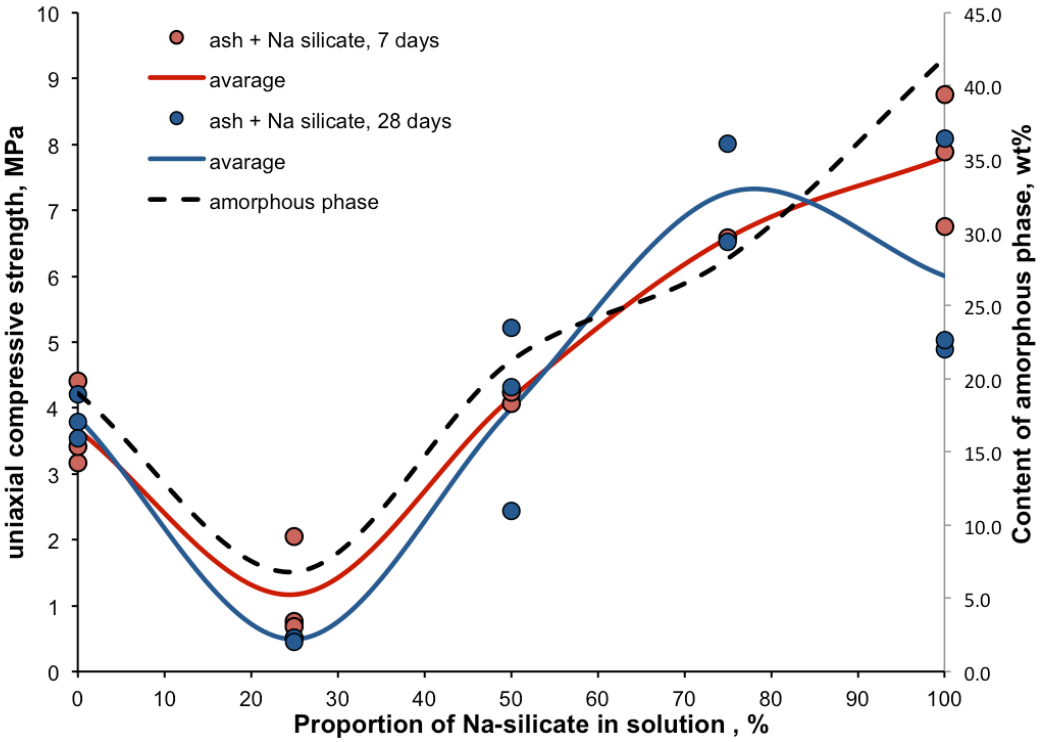

Figure 32. Compressional strength of samples mixed with different proportion Na-silicate solutions after 28 of curing compared with measured amorphous phase.

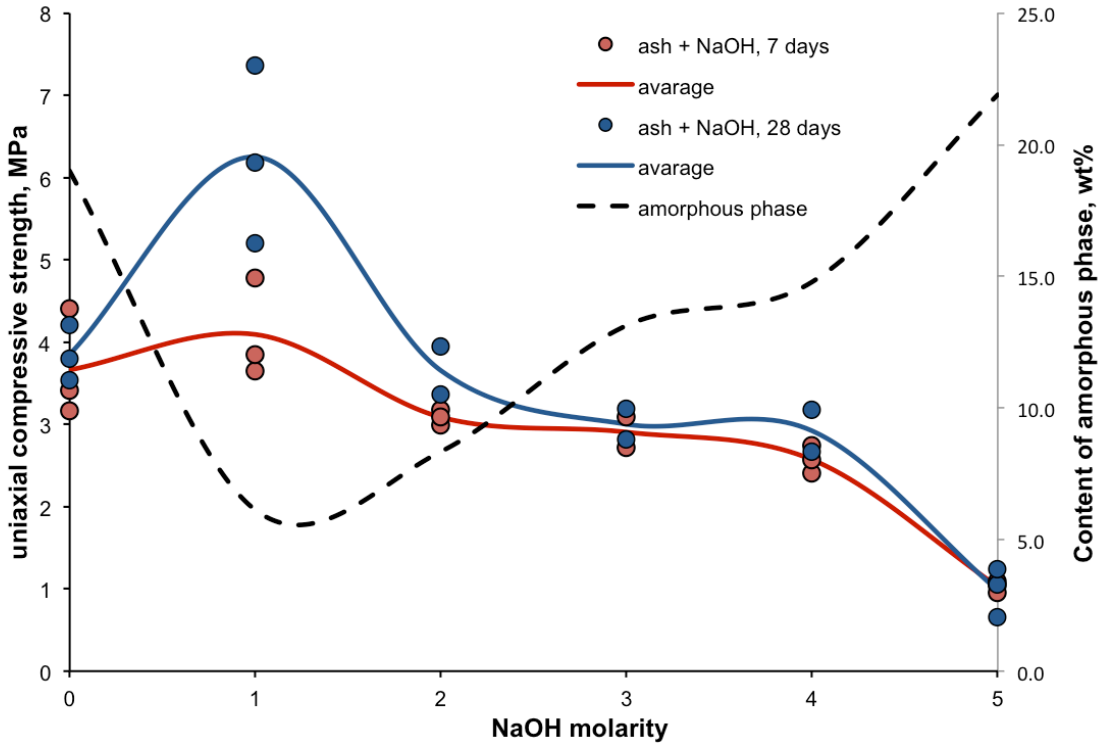

Figure 33. Compressional strength reliance on NaOH molarity after 28 of curing compared with the content of amorphous phase.

Autoclaving had a positive effect on samples mixed with Na-silicate and NaOH, raising compressional strength. The rise in strength could be due to formation of Ca-Al-Si gel that gives true geopolymer its high strength. Nevertheless the true scale of the effect of autoclaving could not be observed because force limit of testing equipment peaks out at 11.8 MPa and samples did not break under this kind of load (Figure 31).

On the other hand autoclaving had a negative effect on the strength and stiffness of samples mixed with 1M NaOH (Figure 30). The main reason for this kind of behavior, could be that ettringite phase, what gives samples the initial high strength and stiffness, could not form or has disappeared after thermal treatment. In SEM images in Figure 34a the ettringite needles are present, but absent in images b, c and d.

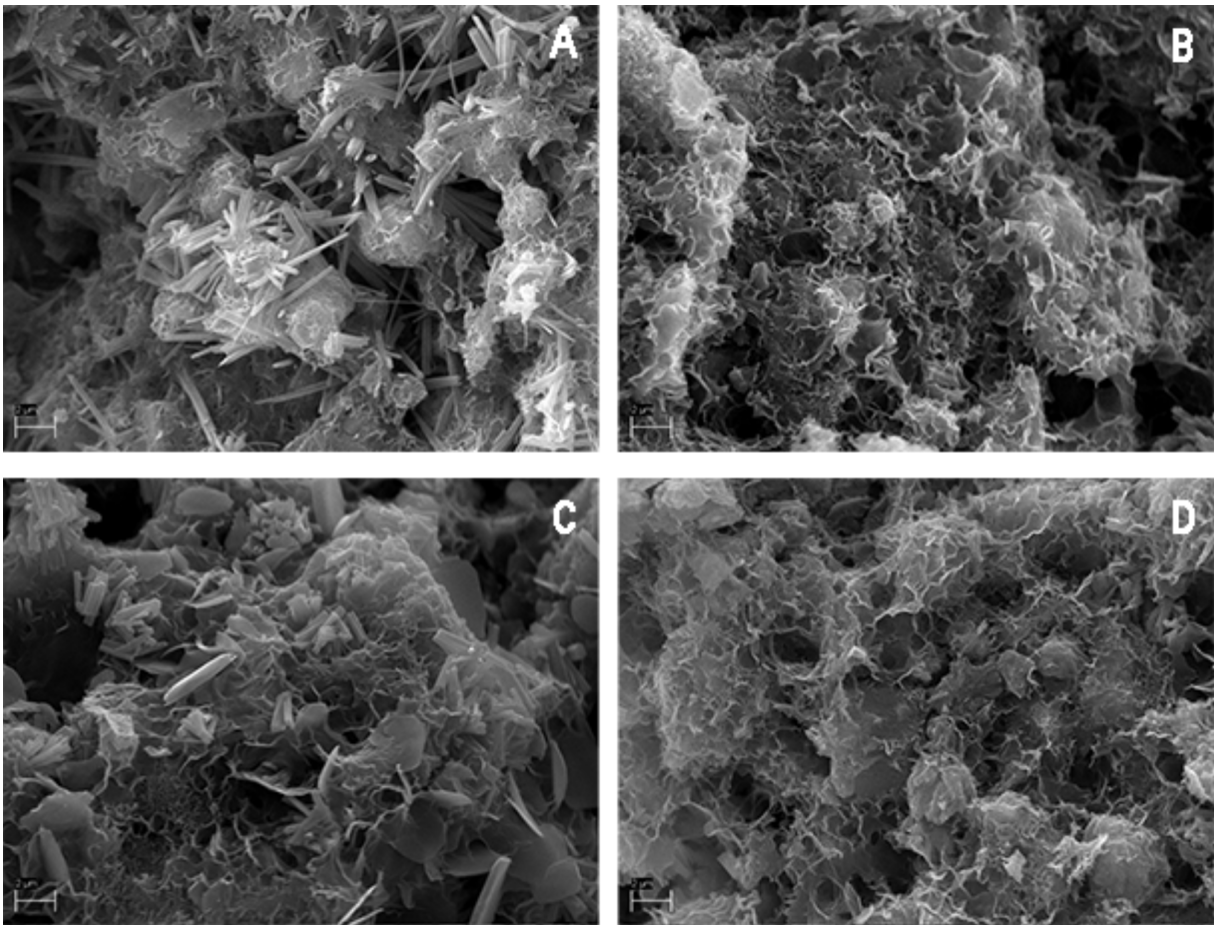

Figure 34. SEM electron images of WHB ash and 1M NaOH mixture, untreated and autoclaved after 28 days. A – untreated ash + 1M NaOH sample, B – autoclaved for 14 hours, C – 24 hours, D – 134 hours.

5.2 Geopolymeric potential of the Enefit 280 WHB ash: theorethical considerations

The Enefit280 WHB ash does not show very good geopolymerization properties, which is evidently related to the characteristics and the content of potentially reactive phases/components. Concerning the reactive components potentially used for geopolymers there is a wide range of possible raw materials. Typically activated clay and/or natural pozzolan materials (Davidovits, 2011) like volcanic ash are considered as primary material for geopolymeric binders. Also, variety of secondary materials like slags and ashes from very different processes can be used (Provis and Bernal, 2014). All these have considerably varying starting compositions and result in large variety of alkali activation reaction products. The "classical" geopolymers are based on aluminosilicate raw materials such as kaolin clay and/or aluminosilicate fly ashes that form upon alkali activation strong alumosilicate polymer networks (Davidovits, 2011). On the other hand, slags with high CaO content develop cementitious calcium-silicate-hydrate (CSH) and calcium-aluminium-hydrate (CAH) phases that are formed in ordinary Portland cement hydration (OPC) (Mijarsh et al., 2015).

Therefore, for achieving and maintaining good strength and chemical resistance/durability of the geopolymeric materials the initial composition and selection of additives and proper activation methods is important. Moreover, the suitability of the material and its estimated final strength upon activation could be estimated from the composition and properties of the raw materials (Aughenbaugh et al., 2015).

In general, the composition of the Estonian oil shale ash produced either in thermal power or in shale oil retorting processes is considerably different form the raw materials typically used for producing geopolymeric binders (Figure 35). By its composition the oil shale ash could be considered as a C-type fly ash that is a Ca-rich ash (CaO content >20 wt%) that can be and are used to produce geopolymers with a considerable final strength (Guo et al., 2010a; Mijarsh et al., 2015). Indeed, the variation of chemical composition of oil shale ashes of different origin agrees (or is somewhat higher) with relative CaO content of several other geopolymer raw materials (Figure 35). However, the Estonian oil shale ashes including the Enefit 280 WHB studied here, are characterized compared with other raw materials by consistently lower proportion of Al_2O_3. This compositional peculiarity by itself dictates that

formation of strong alumosilicate polymer networks does not contribute or is subdued in development of uniaxial strength in Enefit280 WHB ash based systems.

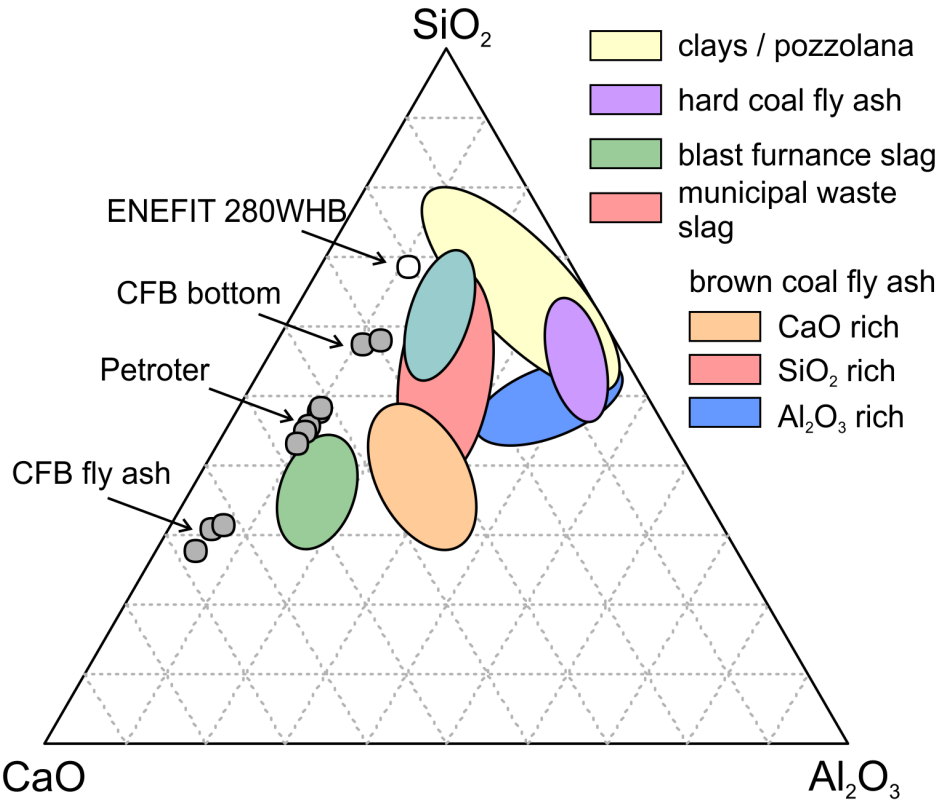

Figure 35. Classification of potential raw materials used for geopolymers on CaO-SiO_2-Al_2O_3 ternary plot. Modified after Buchwald et al. (2005). Data for Petroter ash from Paaver et al. (2016) and oil shale CFB ashes from Bityukova et al. (2010).

If compared with a classification system of geopolymer raw materials developed by Duxson and Provis (2008) then Enefit280 WHB ash as well as other Estonian oil shale ashes fall of the composition fields of other raw materials including (meta)kaolin clay, F- and C-type fly ashes (Figure 36, data for fields from Duxson and Provis, 2008 and Aughenbaugh et al., 2015) mainly because of lower Al content. This classification system for geopolymer aluminosilicate raw materials uses the molar contents of Si, Al, and combined network modifiers based on charge-balancing capacity whereas the network modifier content is used to quantify the relative amount of alkali and alkali earth metals (Ca^{2+}, Mg^{2+}, Na^{+}, K^{+}) present in fly ash (Duxson and Provis, 2008). Alkali elements provide charge-balancing by balancing the negative charge of tetrahedral aluminium that makes aluminum stay in 4-coordination, which has higher solubility than the 6-coordination form. As a result more Al would be

available for geopolymerization and fly ashes with higher network modifying agents generally produce stronger geopolymers (Aughenbaugh et al., 2015). The network modifier content even in the Enefit 280 WHB ash with the lowest CaO among oil shale ashes content in oil shale ash is higher or in the same range as in the raw materials producing the strongest geopolymers, but evidently there is not enough Al available for that (Figure 36).

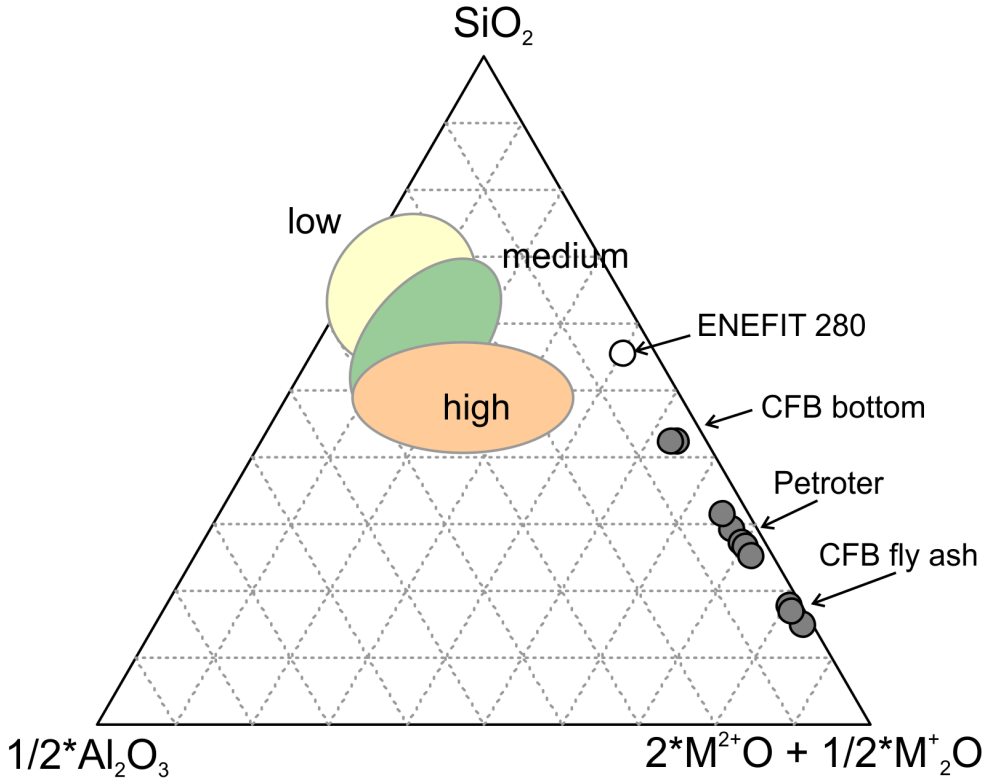

Figure 36. Ternary plot showing the relationship between geopolymer compressive strength and fly ash oxide composition. Modified after Aughenbaugh et al. (2015). Data for Petroter ash from Paaver et al. (2016) and oil shale CFB ashes from Bityukova et al. (2010).

Oh et al. (2015) and Aughenbaugh et al. (2015) developed a method to estimate/predict the compressive strength of the geopolymer as a function of the ash network modifier content. In their experimental studies, as expected, strength generally increased as network modifier content increased. Aughenbaugh et al. (2015) provided an exponential curve ($y = 1.14\ e^{0.067x}$ $R^2 = 0.761$) that was fitted to the averaged 28 day strength of different raw materials with varying network modifier content alkali activated with 8M NaOH. If judged from this relationship then Enefit280 WHB ash would show uniaxial compressive strength about 3 MPa upon activation in strong NaOH solution after 28 days. In this study for the ash activated with 5M NaOH only about 1 MPa strength was achieved, which indicates that the modelled

strength is significantly over-predicted. In is important to notice that for Enefit 280 WHB ash the strength is in fact increased in treatments with solutions at progressively lower NaOH molarities (see Figure 24) and the best results were obtained in treatment with 1M NaOH. Similar over-prediction for geopolymerization strength is also obvious for 5M NaOH activated Petroter black ash (Paaver et al., 2016) and thermal power plant CFB cyclon ash (Paiste et al., 2016). The composition of the last would predict uniaxial strength reaching 17 MPa in alkali activated material after 28 days of curing, however, only 1.3 MPa was observed by Paiste et al. (2016). This suggests that in the oil shale ashes the development of the strength is not limited by the availability of the network modifiers, but the lack of potentially soluble silica and specifically aluminium phases.

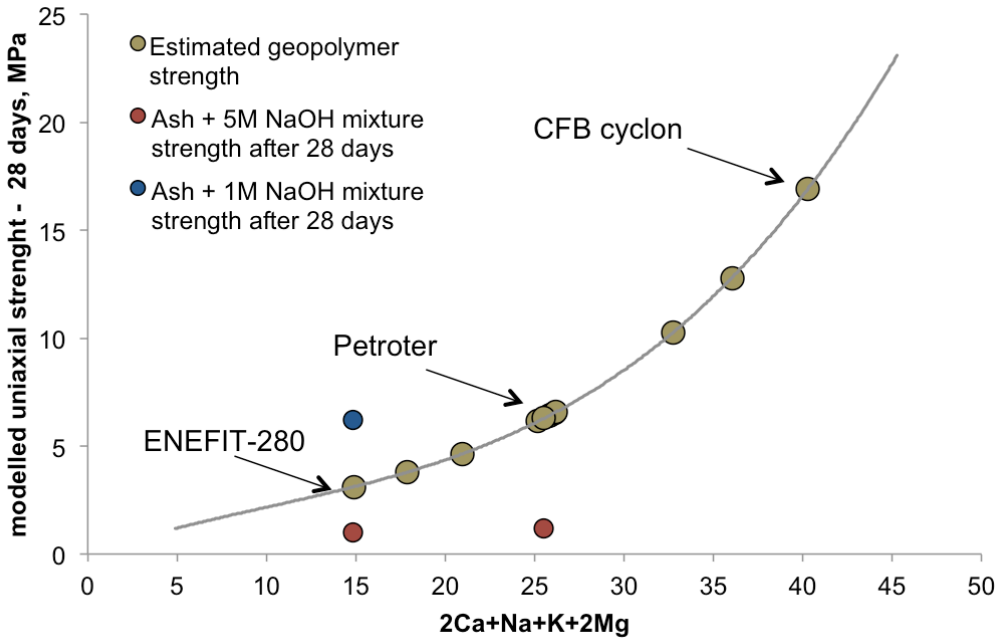

Figure 37. Estimated geopolymer 28-day compressive strength as a function of fly ash network modifier content according to Oh et al. (2015)

Overall, this means that if the oil shale ash (particularly the low temperature processed Enefit ashes) are planned to use for geopolymer production then designing geopolymer mixtures is required to increase the content of available Si and Al in combination with finding an appropriate activator mixed at an optimum ratio.

6. Conclusions

Up to the present day the amounts of the ash residues coming from the Estonian shale oil industry have been relatively small. However, the shale oil producers in Estonia are shifting their focus to a new and more powerful type of SHC retorts, like the Enefit 280 retort and in the near future the share of oil production in the overall turnout of the Estonian oil shale industry will go up, and consequently the amounts of waste ash residue coming from this industry will also rise.

Geopolymeric binders, produced by alkali activation of different solid waste materials that are of rapidly growing interest in building materials research, could be one of the solutions to this waste problem that would give some beneficial use to this industrial waste otherwise landfilled/deposited.

In the current thesis different kind of mortars, using the Enefit 280 waste heat boiler (WHB) ash from the retort built in 2012, were mixed to study and evaluate the potential use of solid heat carrier ash for geopolymer type mortar and cement production. This was done by comparing a series of alkali activated WHB ashes with the self-cementation properties of the same material obtained upon hydration with plain water.

Results of the current study show that fresh WHB ash samples hydrated with plain water achieved a compressional strength up to 3.8 MPa after 7 days of curing, but did not gain any additional strength after 28 days of curing. Samples mixed with 1M NaOH dilution reached the same strength as the ash – water mixtures after 7 days and continued to gain strength during the 28 day curing period reaching up to 7.5 MPa of uniaxial compressive strength. This kind of behavior in strength growth was not observed in samples that were mixed with stronger NaOH solutions. On the contrary, higher molarity of NaOH weakens the samples significantly to a point where the average compressional strength of 1 MPa was measured in samples mixed with 5M NaOH dilution after 28 days. This kind of decrease in strength can be explained by the absence of ettringite phase that is possibly responsible for strength development in the samples mixed with water or 1M NaOH solution. Similarly, the disappearance of ettringite phase could also explain the decrease in strength after 28 days in the 1M NaOH activated samples autoclaved of for 14, 24 and 132 hours at 70 ºC and 2.5 bar

pressure. After autoclaving the strength values measured for these specimens after 28 days of curing dropped on average from 6.25 MPa to 3 MPa.

Na-silicate and Na-silicate/NaOH activated series where the amount of Na-silicate activator was controlled by 25% steps showed a remarkably different strength development as well as mineralogical composition than the samples mixed with water or NaOH. Both of the Na-silicate containing mixtures show high strength values with increasing activator amount whereas it seems that addition of low quantities of activator does not improve the cementation, but results in lower uniaxial strength values compared to ash – plain water mixtures. Nevertheless, samples mixed with higher amounts of activator, supposedly due to the formation of Ca-Na-Al-silicate gel, obtained a relatively high strength reaching up to 11 MPa after 28 days.

Unlike the samples mixed with different molar NaOH solutions, autoclaving had a positive effect on the samples mixed with Na-silicate dilutions as most of the samples could withstand the 11.8 MPa pressure limit of the tester and not break, so the true potential and effect of autoclaving to these mixtures is still to be discovered.

Chemical composition of the Enefit 280 WHB ash as well the composition of other Estonian oil shale processing ashes is compared with other geopolymer raw materials characterized by the same or higher content of CaO but consistently lower proportion of Al_2O_3. This compositional difference suggests that formation of alumosilicate polymer networks typical in geopolymeric binders is subdued in development of uniaxial strength in alkali activated oil shale ash systems. This means that the use of oil shale ash for geopolymer production needs addition of available Si and Al in combination with finding an appropriate activator mixed at an optimum ratio.

Acknowledgements

We wish to express our gratitude to Annete Talpsep and Jaan Aruväli for help with testing and analysis of ash mixtures.

Enefit 280 tahke soojuskandja tuha geopolümeerne potentsiaal

Tänase päevani on põlevkiviõli tööstusest tulenevad tuhajäätmete kogused võrreldes elektrijaamades tekkiva tuhaga võrdlemisi väiksed. Siiski on viimastel aastatel vähenenud põlevkivi kasutamine otsepõletuseks elektrijaamades ja Eesti põlevkiviõli suurtootjad - Eesti Energia ja Viru Keemia Grupp ning Kiviõli Keemiatööstuse OÜ on suuremahuliselt investeerinud õlitootmistehnoloogiasse ja käivitanud või käivitamas uusi suure tootlikkusega tahke soojuskandja tehnoloogiat kasutavaid süsteeme nagu Petroter tehased Viru Keemia Grupp AS-is ja Eesti Energia Enefit 280 tehas. Nende tehastega kaasneb paratamatult ka põlevkiviõli tootmisega tekkivate jäätmete hulga kasv.

Erineva päritoluga tööstuslike jäätmete leeliselisel aktivatsioonil on võimalik toota geopolümeersed sideaineid-tsemente. See valdkond on viimasel ajal kiiresti kerkinud ehitusmaterjalide arendajate huviorbiiti ja need võiksid olla üheks potensiaalsetest kasutusviisidest jäätmetele, mis vastasel juhul leiaksid tee ainult jäätmehoidladesse.

Käesolevas uurimistöös selgitati Enefit 280 jääksoojuskatla tuha sobivust geopolümeeride valmistamiseks. Selleks valmistati Enefit 280 tehasest pärineva tuhaga erinevate segudega katsekehade seeriad. Tekkinud segude omadusi ja geopolümeriseerumist võrreldi sama tuha ja tavalise vee segamisel tekkivate materjalidega

.

Uuringu tulemused näitavad, et kuigi veega segatud proovid saavutasid esimese 7 päevaga arvestava survetugevuse keskmiselt 3.5 MPa, siis pärast 28 päeva kivistumist nende survetugevus ei tõusnud. Samas, 1M NaOHga valmisatud proovide survetugevus tõusis pärast 28 päeva kivistumist keskmiselt kuni 7.5 MPa tasemele. Sellegipoolest vähendas edasine NaOH molaarsuse tõstmine proovide tugevust ning muutusid need pehmemaks ja nõrgemaks nii, et 5M NaOH lahusega aktiveeritud proovide keskmiseks survetugevuseks pärast 28 päeva oli vaid 1 MPa. Sellist tugevuse kaotust võib seletada vee või 1M NaOHga segatud proovides eksisteeriva, kuid tugevama NaOH lahusega valmistatud proovides puuduva etringiidi faasiga, mille nõeljate kristallide liitumisel tekkivad tuhaosakesi siduvad võrgustikud, mis omakorda seovad kogu proovi ühtseks ühendatud massiks.

Etringiidi kadumine termilisel töötlemisel võib olla ka põhjuseks miks 1M NaOHga segatud ja autoklaavitud katsekehad pärast 28 päeva möödumist oma tugevuses hoopis kaotasid. Ilma

autoklaavimiseta katsekehade survetugevus oli pärast 28 päevast tardumist kuni 7.5 MPa ning pärast autoklaavimist keskmiselt 3MPa.

Vesiklaasi (Na-silkaadi lahusega) ning vesiklaasi ja NaOH seguga valmistatud katsekehade seeriad, kus tsementeerumist kontrolliti aktivaatori koguse lisamisega 25% sammudega, olid oma tugevus- ja tsementeerumisomaduselt täiesti erinevad vee või NaOH segatud katsekehadest. Nii vesiklaasi kui vesiklaasi ja NaOH seguga valmistatud katsekehad saavutasid võrdlemisi kõrgeid survetugevuse tulemusi progresseeruvalt suuremate aktivaatori kogustega. Huvitavalt olid katsekehad kus kasutati 25% vesiklaasi võimalikust tuha veesidumisvõimest kokkuvõttes nõrgemad kui veega segatud proovid, samas kui katsekehad kus kasutati massilt 100% vesiklaasi võimalikust tuha veesidumisvõimest saavutasid pärast 28 päeva möödumist tõenäoliselt tänu Ca-Na-Al-silikaat geeli moodustumisele suhteliselt kõrgeid survetugevuse tulemusi, mis ulatusid kuni 11 MPa.

Erinevalt NaOHga segatud katsekehadest mõjus autoklaavimine Na-silikaadiga segatud proovidele positiivselt, kuna enamus autoklaavitud proovidest ostusid tugevamaks kui ilma autoklaavimiseta. Proovide tegelikku survetugevust ei õnnestunud määrata kuna nende kehade tugevus oli suurem kui kasutatud survetugevuse pressi maskimaalne mõõtmispiir – 11.8 MPa ja neid ei olnud võimalik meie laboris purustada. Seega vajab autoklaavimise mõju tugevusele veel edaspidist uurimist.

Võrreldes Enefit 280 tuha ja ka teiste Eesti põlevkivituhkade keemilist koostist maailmas geopolümeeride valmistamiseks kasutatavate toormetega on ilmne, et Eesti põlevkivituhkade CaO sisaldus on nendega sarnane või kõrgem, aga samas on Al_2O_3 sisaldus põlevkivituhkades selgelt madalam. See tähendab, et alumosilikaatsete võrgustike tekkimine, mis on tüüpiliselt iseloomulik geopolümeeridele, on Eesti põlevkivituhkades allasurutud ning vähese mõjuga tugevate tsementeerivate sidemete tekkimiseks. Edaspidistes uuringutes on vaja leida võimalused/viisid leelisaktivatsioonil lahustuva räni ja alumiiniumi sisalduse tõstmiseks segudes ja sobilike aktivaatorite leidmiseks.

References:

Aughenbaugh, K.L., Williamson, T. and Juenger, M.C.G., 2015. Critical evaluation of strength prediction methods for alkali-activated fly ash. Materials and Structures, 48(3): 607-620.

Aarna, I. 2013 Eesti Energia AS, Tallinn, Estonia, A new improved solid heat carrier technology (Enefit 280) for processing of oil shale with different grades

Bauert, H. and Kattai, V., 1997. Kukersite oil shale. In: A. Raukas and A. Teedumäe (Editors), Geology and mineral resources of Estonia. Estonian Academy Publishers, Tallinn, pp. 313-327.

Bityukova, L., Motlep, R. and Kirsimae, K., 2010. Composition of Oil Shale Ashes from Pulverized Firing and Circulating Fluidized-Bed Boiler in Narva Thermal Power Plants, Estonia. Oil Shale, 27(4): 339-353.

Buchwald, A., Dombrowski, K. and Weil, M., 2005. The influence of calcium content on the perfomance of geopolymeric binder especially the resistance against acids, 4th International Conference on Geopolymers, St. Quentin, France, pp. 35-39.

Clark, B.A. and Brown, P.W., 1999. Formation of ettringite from monosubstituted calcium sulfoaluminate hydrate and gypsum. Journal of the American Ceramic Society, 82(10): 2900-2905.

Davidovits, J., 2011. Geopolymer Chemistry and Applications. Institut Géopolymère, Saint-Quentin.

Duxson, P. and Provis, J.L., 2008. Designing Precursors for Geopolymer Cements. Journal of the American Ceramic Society, 91(12): 3864-3869.

Golubev, N., 2003. Solid oil shale heat carrier technology for oil shale retorting. Oil Shale, 20(3): 324-332.

Guo, X.L., Shi, H.S., Chen, L.M. and Dick, W.A., 2010a. Alkali-activated complex binders from class C fly ash and Ca-containing admixtures. Journal of Hazardous Materials, 173(1-3): 480-486.

Guo, X.L., Shi, H.S. and Dick, W.A., 2010b. Compressive strength and microstructural characteristics of class C fly ash geopolymer. Cement & Concrete Composites, 32(2): 142-147.

Kaasik, A., Vohla, C., Motlep, R., Mander, U. and Kirsimae, K., 2008. Hydrated calcareous oil-shale ash as potential filter media for phosphorus removal in constructed wetlands. Water Research, 42(4-5): 1315-1323.

Kearns, J. and Tuohy, E., 2015. Trends in Estonian oil shale utilization: October 2015. Analysis: International Centre for Defence and Security. International Centre for Defence and Security, Tallinn, pp. 22.

Koiv, M., Liira, M., Mander, U., Motlep, R., Vohla, C. and Kirsimae, K., 2010. Phosphorus removal using Ca-rich hydrated oil shale ash as filter material - The effect of different phosphorus loadings and wastewater compositions. Water Research, 44(18): 5232-5239.

Koiv, M., Ostonen, I., Vohla, C., Motlep, R., Liira, M., Lohmus, K., Kirsimae, K. and Mander, U., 2012. Reuse potential of phosphorus-rich filter materials from subsurface flow wastewater treatment filters for forest soil amendment. Hydrobiologia, 692(1): 145-156.

Kuusik, R., Uibu, M. and Kirsimae, K., 2005. Characterization of oil shale ashes formed at industrial-scale CFBC boilers. Oil Shale, 22(4): 407-419.

Kuusik, R., Uibu, M., Kirsimae, K., Motlep, R. and Meriste, T., 2012. Open-Air Deposition of Estonian Oil Shale Ash: Formation, State of Art, Problems and Prospects for the Abatement of Environmental Impact. Oil Shale, 29(4): 376-403.

Li, Q., Xu, H., Li, F.H., Li, P.M., Shen, L.F. and Zhai, J.P., 2012. Synthesis of geopolymer composites from blends of CFBC fly and bottom ashes. Fuel, 97: 366-372.

Liira, M., Kirsimae, K., Kuusik, R. and Motlep, R., 2009a. Transformation of calcareous oil-shale circulating fluidized-bed combustion boiler ashes under wet conditions. Fuel, 88(4): 712-718.

Liira, M., Koiv, M., Mander, U., Motlep, R., Vohla, C. and Kirsimae, K., 2009b. Active Filtration of Phosphorus on Ca-Rich Hydrated Oil Shale Ash: Does Longer Retention Time Improve the Process? Environmental Science & Technology, 43(10): 3809-3814.

Liive, S., 2007. Oil shale energetics in Estonia. Oil Shale, 24(1): 1-4.

Mijarsh, M.J.A., Johari, M.A.M. and Ahmad, Z.A., 2015. Effect of delay time and Na2SiO3 concentrations on compressive strength development of geopolymer mortar synthesized from TPOFA. Construction and Building Materials, 86: 64-74.

Mindess, S., Young, J.F. and Darwin, D., 2003. Concrete. Prentice Hall, Pearson Education, Inc., Upper Saddle River, NJ, 644 pp.

Motlep, R., Kirsimae, K., Talviste, P., Puura, E. and Jurgenson, J., 2007. Mineral composition of Estonian oil shale semi-coke sediments. Oil Shale, 24(3): 405-422.

Motlep, R., Sild, T., Puura, E. and Kirsimae, K., 2010. Composition, diagenetic transformation and alkalinity potential of oil shale ash sediments. Journal of Hazardous Materials, 184(1-3): 567-573.

Oh, J.E., Jun, Y., Jeong, Y. and Monteiro, P.J.M., 2015. The importance of the network-modifying element content in fly ash as a simple measure to predict its strength potential for alkali-activation. Cement & Concrete Composites, 57: 44-54.

Ots, A., 2006. Oil shale fuel combustion. Tallinna Raamatutrükikoda, Tallinn, 833 pp.

Paaver, P., Paiste, P. and Kirsimäe, K., 2016. Geopolymeric potential of the Estonian oil shale solid residues: Petroter solid heat carrier retorting ash. Oil Shale, submitted.
Paiste, P., Liira, M., Heinmaa, I., Vahur, S. and Kirsimäe, K., 2016. Alkali activated construction materials: alternative use for oil shale processing solid wastes. Construction and Building Materials, in revision.
Pets, L., Knot, P., Haldna, J., Shvenke, G. and Juga, R., 1985. Trace elements in kukersite oil shale ash of Baltic Power Plant. Oil Shale, 2: 379–390.
Pihu, T., Arro, H., Prikk, A., Rootamm, R., Konist, A., Kirsimae, K., Liira, M. and Motlep, R., 2012. Oil shale CFBC ash cementation properties in ash fields. Fuel, 93(1): 172-180.
Provis, J.L. and Bernal, S.A., 2014. Geopolymers and Related Alkali-Activated Materials. Annual Review of Materials Research, 44: 299-327.
Sedman, A., Talviste, P. and Kirsimae, K., 2012a. The Study of Hydration and Carbonation Reactions and Corresponding Changes in the Physical Properties of Co-Deposited Oil Shale Ash and Semicoke Wastes in a Small-Scale Field Experiment. Oil Shale, 29(3): 279-294.
Sedman, A., Talviste, P., Motlep, R., Joeleht, A. and Kirsimae, K., 2012b. Geotechnical characterization of Estonian oil shale semi-coke deposits with prime emphasis on their shear strength. Engineering Geology, 131: 37-44.
Soone, J. and Doilov, S., 2003. Sustainable utilization of oil shale resources and comparison of contemporary technologies used for oil shale processing. Oil Shale, 20(3): 311-323.
Subaer van Riessen, A., 2006. Thermo-mechanical and microstructural characterisation of sodium-poly(sialate-siloxo) (Na-PSS) geopolymers. Journal of Materials Science, 42(9): 3117-3123.
Zhang, Z.H., Wang, H., Zhu, Y.C., Reid, A., Provis, J.L. and Bullen, F., 2014. Using fly ash to partially substitute metakaolin in geopolymer synthesis. Applied Clay Science, 88-89: 194-201.
Talviste, P., Sedman, A., Motlep, R. and Kirsimae, K., 2013. Self-cementing properties of oil shale solid heat carrier retorting residue. Waste Management & Research, 31(6): 641-647.

Supplements

Table 1. Mineral composition (wt%) of NaOH treated samples. t%; tr – trace amount |<0.5%

	Enefit280	ash + water		ash + 1M NaOH		ash + 2M NaOH		ash + 3M NaOH		ash + 4M NaOH		ash + 5M NaOH	
phase/molarity	original	7	28	7	28	7	28	7	28	7	28	7	28
Quartz	8.1	14.4	13.9	13.6	13.6	12.6	13.5	11.7	12.6	11.6	12.4	6.4	11.1
Orthoclase	7.7	13.1	12.4	12.0	12.0	12.3	11.9	10.7	12.3	10.4	11.4	8.2	8.8
Mica/Illite	6.9	12.9	7.7	12.2	12.2	8.0	8.3	7.4	8.0	8.5	8.2	5.9	9.1
Calcite	44.5	32.6	32.1	32.0	32.0	29.0	31.9	28.3	29.0	28.3	29.9	15.0	24.5
Vaterite	1.1	0.6	0.5	0.8	0.8	0.8	1.6	1.1	0.8	2.1	1.6	0.5	1.7
Dolomite	1.0	3.3	2.9	3.6	3.6	1.9	3.0	1.8	1.9	0.9	0.8	1.9	1.9
Portlandite	1.3	tr		tr	tr	3.7	1.5	4.0	3.7	5.8	5.4	0.8	3.6
Periclase	1.0	1.5	0.7	1.4	1.4	0.5	0.8	0.7	0.5	0.5	0.4	1.1	0.4
C2S	3.8	3.3	2.5	3.5	3.5	3.6	4.2	3.8	3.6	3.1	2.9	3.3	3.2
Merwinite	2.8	1.5	1.0	1.8	1.8	2.2	1.9	1.8	2.2	1.1	1.3	1.8	1.4
Wollastonite	1.0	1.0	0.8	1.1	1.1	0.7	0.5	0.5	0.7	0.6	0.5	3.1	1.3
anhydrite	1.2	0.7	0.8										tr
Hydrocalumite		3.7	0.4	6.0	6.0	7.6	8.8	7.1	7.6	5.5	6.6	0.8	8.4
Ettringite		1.4	2.0			1.1		1.0	1.1	2.4	2.0	1.0	0.5
Akermanite	3.5	2.1	0.7	3.2	3.2	1.4	1.8	1.4	1.4	0.1	tr	1.4	0.8
Hematite	1.0	2.1	2.1	1.9	1.9	0.9	1.1	0.9	0.9	0.9	1.0	0.6	1.0
Magnetite	tr	tr	tr	tr	tr	0.6	0.6	tr	0.6	tr	tr	tr	
Amorphous	14.3	5.8	19.0	6.1	6.1	13.1	8.3	17.4	13.1	18.0	14.8	48.0	21.9

Table 2. Mineral composition (wt%) of Na-silicate and Na-silicate/NaOH treated samples. t%; tr – trace amount |<0.5%

	ash + Na-silicate								ash + Na-silicate + NaOH							
	25% dilution		50% dilution		75% dilution		100% dilution		25% dilution		50% dilution		75% dilution5		100% dilution	
phase/days	7	28	7	28	7	28	7	28	7	28	7	28	7	28	7	28
Quartz	14.0	14.0	12.9	12.4	12.4	11.4	12.2	8.5	11.8	13.8	13.2	12.8	10.9	10.9	11.8	7.1
Orthoclase	13.6	12.9	12.2	12.1	10.9	11.0	11.6	8.8	11.6	12.4	12.5	11.1	10.4	10.3	11.6	6.3
Mica/Illite	10.3	11.7	9.0	8.7	9.7	7.2	13.1	8.1	7.1	9.7	8.1	10.5	6.4	6.3	7.1	4.5
Calcite	33.4	32.8	29.7	30.2	28.9	26.7	24.9	19.5	26.2	31.2	28.5	29.5	25.3	25.4	26.2	14.9
Vaterite	2.0	1.3	2.4	1.5	0.8	1.1	3.0	1.3	1.0	1.6	1.9	1.6	1.1	1.1	1.0	0.8
Dolomite	2.9	2.6	2.8	2.6	2.8	2.8	0.6	1.6	2.4	2.4	2.4	2.8	2.6	2.7	2.4	2.1
Portlandite					tr	tr	8.8	tr	tr		tr	tr			tr	0.5
Periclase	2.2	1.9	2.0	1.6	2.0	1.1	0.4	1.5	1.9	1.6	1.8	1.5	1.4	1.4	1.9	1.1
C2S	3.3	3.1	4.3	2.3	3.4	2.0	5.0	1.6	3.1	3.0	3.5	2.3	2.2	2.2	3.1	1.9
Merwinite	2.4	1.6	2.2	1.2	2.0	1.3	2.0	1.8	2.0	1.9	2.6	2.1	1.7	1.6	2.0	1.7
Wollastonite	0.7	1.1	0.8	1.3	3.1	1.5	3.0	0.7	0.6	0.8	0.8	0.5	0.9	0.8	0.6	2.8
Anhydrite		1.5							1.9	5.1	3.9		2.1	2.1	1.9	
Hydrocalumite	3.7	3.5	3.9	1.0	1.9	1.0	5.8	0.5	3.0	3.4	3.2	2.3	1.8	1.7	3.0	
Ettringite	tr	tr	0.6	tr		0.5	1.2	0.9	tr	tr	tr	0.7			tr	1.9
Akermanite	2.2	2.4	2.0	1.5	2.7	2.0	1.4	1.3	1.5	2.1	2.0	0.9	1.8	1.7	1.5	0.9
Hematite	1.8	1.9	1.8	1.4	1.3	1.5	1.1	1.1	1.5	1.7	1.6	1.6	1.4	1.4	1.5	0.7
Magnetite	0.6	tr	tr	0.5	0.6	0.5	0.5	tr	0.6	0.5	0.6	0.5	tr	tr	0.6	
Amorphous	6.3	6.8	12.7	21.2	17.0	28.2	5.4	41.9	23.2	8.0	12.8	19.1	29.2	29.6	23.2	52.5

Table 3. Mineral composition (wt%) of autoclaved samples. t%; tr – trace amount |<0.5%.

	Ash + 1M NaOH			ash + Na silicate + NaOH		
phase/hours	14H	24H	134H	14H	24H	134H
Quartz	13.5	12.7	12.2	12.7	11.5	13.7
Orthoclase	11.2	11.2	10.9	11.2	10.9	11.8
Mica/Illite	7.3	6.7	8.9	6.7	7.0	8.5
Calcite	31.7	29.1	31.4	29.1	28.5	34.6
Vaterite	0.5	0.7	2.2	0.7	0.6	2.5
Dolomite	3.1	2.4	2.5	2.4	3.2	3.3
Portlandite			tr.		0.5	tr.
Periclase	0.7	0.8	0.5	0.8	1.1	0.6
C2S	3.0	2.7	3.1	2.7	2.4	3.6
Merwinite	1.5	1.1	1.4	1.1	1.1	1.2
Wollastonite	1.3	1.0	1.5	1.0	3.2	1.8
Anhydrite	tr	0.5	0.6	0.5		0.7
Hydrocalumite	6.6	5.7	6.1	5.7	2.3	7.2
Ettringite						
Akermanite	1.5	1.6	1.7	1.6	1.8	2.6
Hematite	1.8	1.7	1.6	1.7	1.6	1.8
Magnetite	0.4	0.4	0.5	0.4	0.5	0.6
Amorphous	15.5	21.6	14.6	21.6	23.8	5.5

Table 4. Chemical composition (wt%) of NaOH treated samples.

sample/oxide	SiO2	Al2O3	TiO2	Fe2O3	MnO	CaO	MgO	Na2O	K2O	P2O5	SO3	L.O.I.
Original ash	43.22	7.72	0.31	2.93	0.03	19.66	3.17	0.06	2.44	0.09	2.25	17.65
H20, 7 days	33.68	6.69	0.35	3.57	0.06	22.79	3.45	0.10	2.58	0.10	4.54	21.53
H2O 28 days	34.14	6.91	0.33	3.49	0.04	22.23	3.35	0.19	2.58	0.10	4.63	21.39
1M NaOH,7 days	33.12	6.59	0.33	3.48	0.06	22.51	3.10	1.24	2.56	0.10	3.96	22.34
1M NaOH,28 days	34.64	6.83	0.32	3.46	0.05	22.62	2.87	1.38	2.62	0.10	4.05	20.38
2M NaOH,7 days	32.46	6.48	0.32	3.37	0.04	21.92	2.67	3.10	2.54	0.10	3.82	22.52
2M NaOH,28 days	33.23	6.69	0.33	3.32	0.04	21.49	2.56	3.08	2.55	0.10	3.79	22.20
3M NaOH,7 days	32.42	6.37	0.32	3.34	0.04	21.74	2.53	4.17	2.52	0.10	3.42	22.39
3M NaOH,28 days	32.05	6.25	0.34	3.44	0.04	22.10	2.62	4.31	2.55	0.10	3.52	22.07
4M NaOH,7 days	32.29	6.31	0.32	3.27	0.04	21.28	2.41	5.24	2.51	0.10	3.30	22.37
4M NaOH,28 days	31.21	5.98	0.32	3.31	0.04	21.76	2.51	5.47	2.47	0.10	3.55	22.75
5M NaOH,7 days	49.25	4.08	0.24	2.37	0.03	14.93	1.87	5.53	1.75	0.07	1.92	17.53
5M NaOH,28 days	31.41	6.03	0.32	3.22	0.05	20.27	2.28	7.99	2.41	0.09	3.23	22.11

Table 5. Chemical composition (wt%) of Na-silicate and Na-silicate/NaOH treated samples.

sample/oxide	SiO2	Al2O3	TiO2	Fe2O3	MnO	CaO	MgO	Na2O	K2O	P2O5	SO3	L.O.I.
original ash	43.22	7.72	0.31	2.93	0.03	19.66	3.17	0.06	2.44	0.09	2.25	17.65
Na-silicate 25%, 7 days	35.95	6.24	0.32	3.36	0.05	22.39	3.07	0.91	2.50	0.10	3.34	21.28
Na-silicate 25%, 28 days	36.39	6.36	0.33	3.34	0.04	21.98	2.89	0.97	2.51	0.10	3.30	21.24
Na-silicate 50%, 7 days	37.51	6.18	0.32	3.26	0.04	21.83	3.14	1.06	2.49	0.10	3.46	19.90
Na-silicate 50%, 28 days	38.54	5.87	0.30	3.11	0.05	20.56	2.70	2.21	2.40	0.09	2.50	21.14
Na-silicate 75%, 7 days	39.70	5.31	0.28	2.83	0.03	18.78	2.50	4.45	2.20	0.09	2.80	20.46
Na-silicate 75%, 28 days	40.02	5.30	0.27	2.95	0.05	19.38	2.61	3.81	2.24	0.09	2.31	20.49
Na-silicate 100%, 7 days	30.41	5.78	0.32	3.14	0.04	20.05	2.31	8.75	2.35	0.09	3.73	22.48
Na-silicate 100%, 28 days	49.53	4.15	0.23	2.36	0.04	14.70	1.74	5.85	1.77	0.07	2.06	17.00
Na-silicate 25%+ NaOH, 7 days	38.03	5.84	0.30	3.00	0.04	20.12	2.64	2.33	2.34	0.09	2.57	22.16
Na-silicate 25%+ NaOH, 28 days	37.32	6.11	0.31	3.22	0.04	21.32	2.98	1.03	2.49	0.10	3.32	21.20
Na-silicate 50%+ NaOH, 7 days	40.23	5.66	0.28	2.97	0.05	19.66	2.58	2.49	2.31	0.09	3.16	19.91
Na-silicate 50%+ NaOH, 28 days	39.19	6.08	0.32	3.14	0.04	20.88	2.83	1.62	2.45	0.09	3.27	19.51
Na-silicate 75%+ NaOH, 7 days	43.97	5.19	0.27	2.71	0.03	17.71	2.30	3.39	2.14	0.08	2.58	19.10
Na-silicate 75%+ NaOH, 28 days	43.58	5.31	0.26	2.68	0.04	17.30	2.15	3.65	2.16	0.08	2.70	19.54
Na-silicate 100%+ NaOH, 7 days	42.02	3.32	0.22	2.32	0.03	15.09	1.89	12.37	1.62	0.06	2.55	18.11
Na-silicate 100%+ NaOH, 28 days	43.08	3.44	0.23	2.32	0.03	15.23	1.89	12.04	1.66	0.06	2.79	16.94

Table 6. Chemical composition (wt%) of autoclaved samples.

sample/oxide	SiO2	Al2O3	TiO2	Fe2O3	MnO	CaO	MgO	Na2O	K2O	P2O5	SO3	L.O.I.
original ash.	43.22	7.72	0.31	2.93	0.03	19.66	3.17	0.06	2.44	0.09	2.25	17.65
Na-silicate 50%+ NaOH, 28 days, autoclaved 14H	39.16	5.39	0.29	3.08	0.04	20.16	2.62	4.24	2.28	0.09	2.88	19.24
Na-silicate 50%+ NaOH, 28 days, autoclaved 24H	38.98	5.34	0.28	3.11	0.07	20.45	2.66	4.10	2.29	0.09	2.76	19.32
Na-silicate 50%+ NaOH, 28 days, autoclaved 134H	33.86	6.48	0.33	3.53	0.04	22.54	3.02	1.72	2.61	0.10	4.31	20.86
1M NaOH, 28 days, autoclaved 14H	32.84	6.33	0.34	3.56	0.05	22.97	3.07	1.73	2.62	0.10	4.31	21.47
1M NaOH, 28 days, autoclaved 24H	33.31	6.46	0.34	3.50	0.05	22.64	2.94	1.81	2.63	0.10	4.38	21.25
1M NaOH, 28 days, autoclaved 134H	33.36	6.35	0.33	3.55	0.06	22.91	2.96	1.80	2.62	0.10	4.29	21.05
1M NaOH, 28 days, 45% saturation	34.46	6.59	0.35	3.89	0.04	24.64	3.40	1.26	2.77	0.11	4.28	17.36
1M NaOH, 28 days, 50% saturation	33.44	6.53	0.34	3.53	0.06	22.97	3.10	1.30	2.62	0.10	4.14	21.25
Na-silicate 50%+ NaOH, 28 days, 45 saturation	38.16	5.62	0.29	3.21	0.04	21.14	2.91	3.29	2.41	0.10	3.10	19.17
Na-silicate 50%+ NaOH, 28 days 50% saturation	37.56	5.65	0.31	3.22	0.06	21.16	2.89	3.14	2.42	0.09	3.19	19.68

Non-exclusive licence to reproduce thesis and make thesis public

I, Peeter Paaver

1. herewith grant the University of Tartu a free permit (non-exclusive licence) to:

1.1. reproduce, for the purpose of preservation and making available to the public, including for addition to the DSpace digital archives until expiry of the term of validity of the copyright, and

1.2. make available to the public via the web environment of the University of Tartu, including via the DSpace digital archives until expiry of the term of validity of the copyright,

Geopolymeric potential of the Enefit 280 oil shale solid heat carrier retorting ash

supervised by Kalle Kirsimäe and Päärn Paiste

2. I am aware of the fact that the author retains these rights.

3. I certify that granting the non-exclusive licence does not infringe the intellectual property rights or rights arising from the Personal Data Protection Act.

Tartu, **20.05.2016**